UNIVERSITAT DE BARCELONA

DEPARTAMENT DE PREHISTÒRIA, HISTÒRIA ANTIGA I ARQUEOLOGIA

PROGRAMA DE DOCTORAT

"ESTRUCTURES SOCIO-ECONÒMIQUES A LA PREHISTÒRIA I MÓN ANTIC"

BIENNI 1994-1996

STUDY OF ASH LAYERS THROUGH PHYTOLITH ANALYSES FROM THE MIDDLE PALEOLITHIC LEVELS OF KEBARA AND TABUN CAVES.

TESI PER OPTAR AL TÍTOL DE DOCTOR EN GEOGRAFIA I HISTÒRIA (PREHISTÒRIA, HISTÒRIA ANTIGA I ARQUEOLOGIA)

Presentada per: **Rosa Maria Albert Cristóbal**

Dirigida per: **Josep Maria Fullola Pericot**

Steve Weiner

Linda Scott Cummings

Barcelona, 1999

5.2 - PHYTOLITH ANALYSIS OF LAYERS B AND C FROM TABUN CAVE

A) Introduction

Tabun cave is located on Mt. Carmel, about 20 km south of Haifa (Israel). The entrance faces northwest overlooking the Mediterranean coastal plain about 45 m above sea level. The cave is divided into 3 chambers: the outer one now without a roof, the inner chamber with a roof that contains a large "chimney" about 5 m in diameter, and an intermediate chamber connecting the two (Figure 17).

Tabun cave was first excavated by Dorothy Garrod between 1929 and 1934 (Garrod & Bate, 1937), and after that by Arthur Jelinek from 1967 to 1972 (Jelinek et al., 1973; Jelinek, 1982). Excavations of mainly the lowermost layers are currently ongoing by Avraham Ronen.

Figure 17 - Photograph of Tabun cave. Detail of the entrance showing the stratigraphic sequence of the cave.

The sediments in Tabun Cave accumulated from the Late Acheulian (Jelinek et al., 1973) to historic times. In the excavations carried out by Garrod and Bate (1937) they divided the section into 7 levels (A - G), based mainly on cultural differences. Jelinek et al. (1973) regrouped the levels into three geological units (Units I, II and III), reflecting the fact that the sediments in the upper two levels are markedly different from those in the underlying levels (Goldberg, 1973; Farrand 1979, 1994). Unit I is equivalent to Level B, Unit II to Level C and Unit III to all the underlying levels.

The sediment in Level B or Unit I was deposited during the late Mousterian and comprises mainly a reddish brown clay that closely resembles the terra rossa soil in the region (Brammall in Garrod & Bate, 1937) with abundant limestone boulders, and little or no bedding (Garrod & Bate, 1937). Weiner et al. (1995) observed that many of the angular limestone blocks buried in the sediment have reaction rims, which are composed of carbonated apatite. Dating of teeth by ESR (Electron Spin Resonance) indicates that the age of this level is around 80,000 years old (Grun, Stringer & Schwarcz, 1991) while

uranium series dating also of teeth indicate that Level B is about 50,000 years old (McDermott et al., 1993).

Level C (Unit II) underlies Level B, except locally in the extant section, which is about 2.5 m thick and where Level B sediments have, in places, filled a channel that eroded into Level C (Figure 18). Level C differs from Level B mainly due to the presence of abundant white lenses interspersed between layers of reddish brown sediments similar to those of the overlying unit. From a distance, the white lenses appear to extend continuously for several meters (Jelinek et al., 1973). Close examination of the Level C sediments exposed in the west section of square 6, as excavated by Jelinek et al. (1973), reveals a finely bedded alternating sequence of white, brown and black layers (Figure 19). The lateral extent of the layers is limited (generally to less than 50 cm), and except for local reworking due to burrowing, the fine-scale structures observed appear to be intact (Figure 20). Many of these are lens-shaped structures that resemble hearths in cross-section.

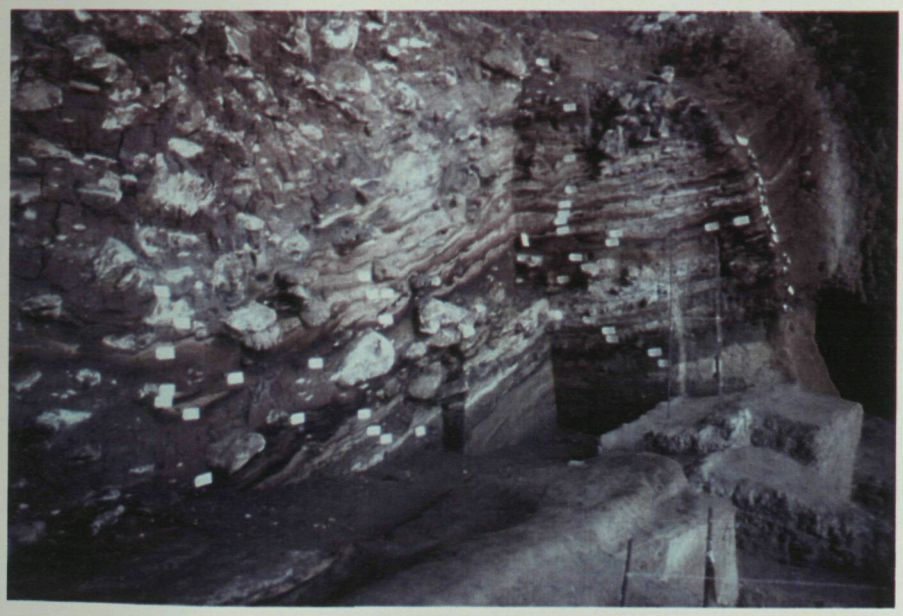

Figure 18 - Photograph of Levels B and C from Tabun cave during the excavation by Jelinek, showing the distinctively layered stratigraphy of Level C overlain by the massive Level B sediments and abundant angular limestone blocks. The contact between level C and Level B at this location is clearly erosional. From this view the layers of level C appear to extend over several meters.

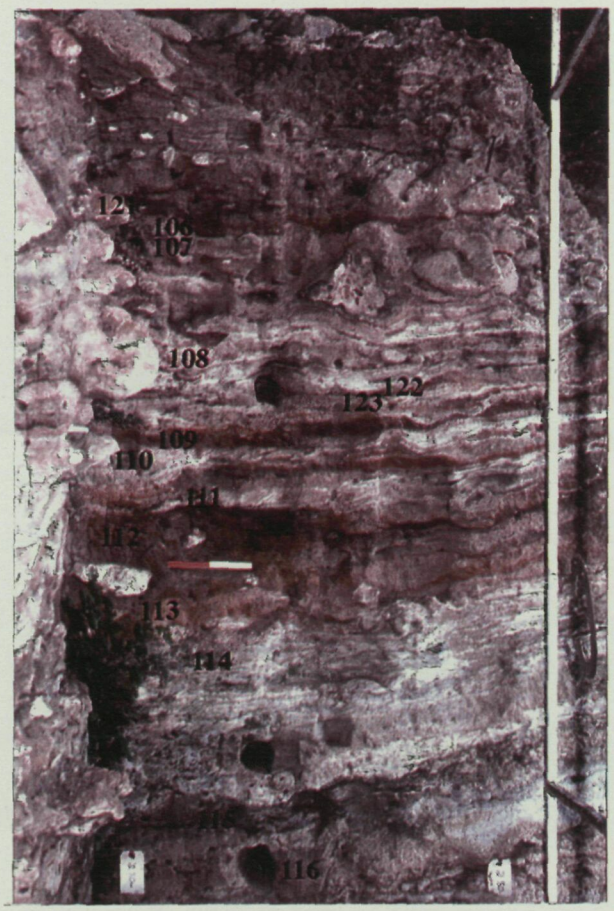

Figure 19 - Photograph of the Level C of Tabun cave. Sediments showing the finely bedded alternating sequence of brown, black and white layers. The numbers designate the locations of the samples studied. The section is from excavation square 6 (See figure 2). Scale bar: 10 cm intervals.

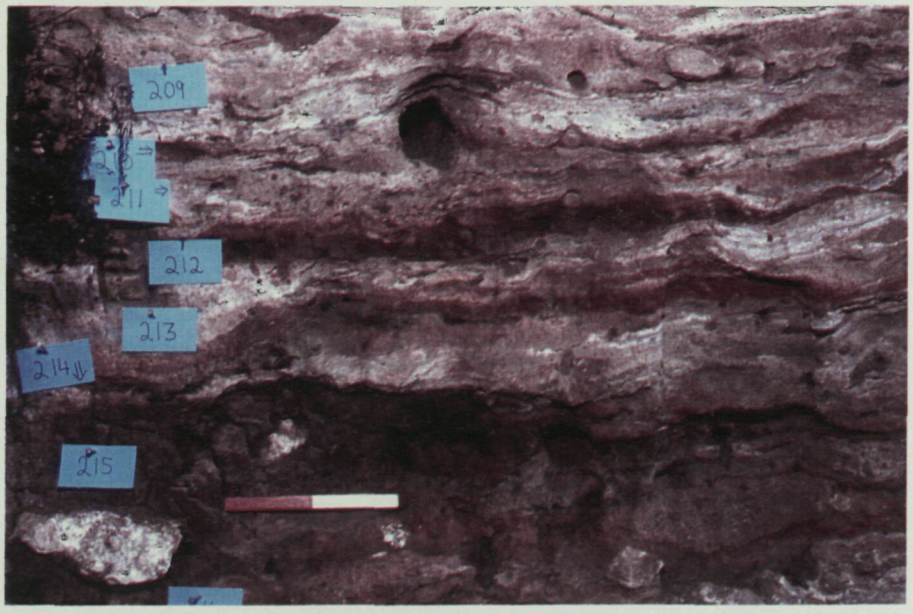

Figure 20 - Photograph of the sediments in Level C showing the brown, black and white layers. Note in particular the fine-scale layered structure within each of the layers. Scale bar: 10 cm intervals.

Thermoluminescence (TL) dating indicates that the average age of this unit is about 170,000 years (Mercier et al., 1995). This age estimate is considerably older than the roughly 100,000 and 125,000 years ages obtained by uranium series (McDermott et al., 1993) and ESR dating (Grun, Stringer & Schwarcz, 1991) respectively.

Below Level C there is a very thick sequence (Unit III) that shows some bedding and appreciable amounts of authigenic phosphate minerals. A gradational decrease in the proportion of clay-sized sediments from the top to the bottom was observed, with a concurrent increase in sand-sized quartz grains mainly of aeolian origin, and enhanced by the proximity of the sea (Bull & Goldberg, 1985; Tsatskin, Weinstein-Evron & Ronen, 1995). TL dating of the middle part of this section shows that it is at least 350,000 years old (Mercier et al., 1995).

The section through these layers (Figure 21) as depicted by Garrod and Bate (1937), shows that Level B markedly decreases in thickness from the inside of the cave to the outside suggesting that the source of the sediments is the chimney located in the inner chamber. The presence of many angular blocks of limestone in the sediment is due to the widening of the chimney (Garrod & Bate, 1937). Level C also decreases in thickness, but to a lesser extent than Level B. This resemblance of the sediment and the presence of angular limestone blocks appearing for the first time at the base of Level C, prompted Jelinek et al. (1973) to conclude, that the chimney opened at the beginning of Tabun C, and increased significantly in size during the Tabun B period.

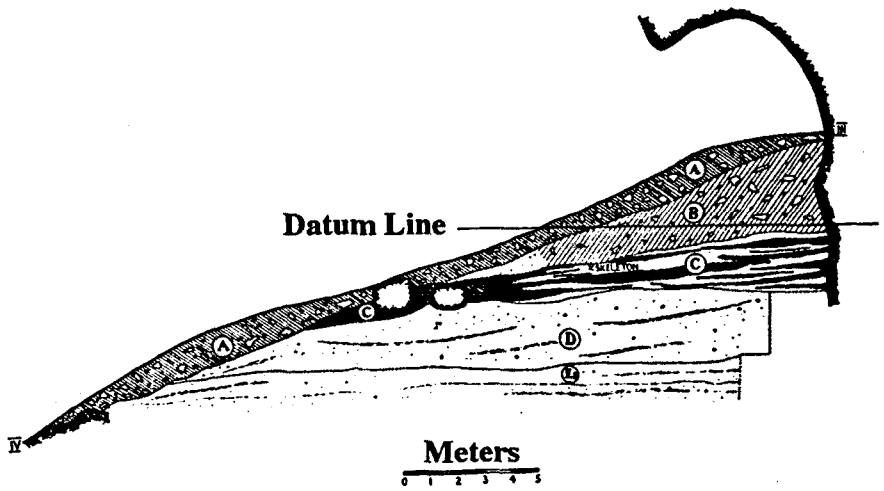

Figure 21 - Stratigraphic section through Levels A to D showing that the thickness of Levels B and C decrease from inside the cave towards the talus slope. The position of the datum line from which all the sample elevation levels are measured is also shown. The Figure is adapted from Plate XXX drawn by Garrod and Bate (1937).

With respect to the archaeological finds, Garrod and Bate (1937) noted that in Level B flints were not very abundant, but the proportion of finished implements was high compared to the underlying levels. Furthermore, the bones present in Level B are representative of a modern fauna. Unlike the bones in Level C are predominantly derived from *Dama mesopotamica.* Garrod and Bate (1937) inferred from this faunal analysis that a major climatic change occurred during the transition from Level C to Level B, with an increase in rainfall and tree cover. They noted that complete specimens, with broken bones, and associated limb bones were more common in Level B than in the underlying layers, which would suggest that part of the fauna could have accumulated "in the form of carcasses violently washed in" (p. 150, Garrod & Bate, 1937). They also noted the presence of a number of small hearths in the outer chamber, but elsewhere there was no trace of hearth material. For Jelinek et al. (1973) this scenario suggested that during the Tabun B period, the cave was used as a specialized butchering station and not for normal domestic activities. In fact Jelinek et al. (1973) proposed that the chimney was used as a natural game trap.

The abundant white and brown/black layers (Figures 19 & 20) present in Level C were described by Garrod and Bate (1937) as hearths, and they noted the presence of many flints and debitage cracked by fire. Animal bones are from a diverse array of species and are more abundant on the talus (entrance of the cave). Most are black and many show signs that they were broken for food. All these observations are consistent with the cave being used as a domestic occupation site (Garrod & Bate, 1937). The cementum analyses of gazelle teeth (Lieberman 1993) show that gazelles were killed during this period in the winter, reflecting perhaps a seasonal mode of winter occupation. Jelinek et al. (1973) noted that many of the ash layers could be traced from wall to wall over a distance of some 8 to 10 m and concluded that they were not hearths, but must have been formed due to repeated fires that engulfed the cave interior. They surmised that Garrod and Bate did not observe this phenomenon because they excavated the areas closer to the cave entrance. Albert et al. (1999a) also observed, that the white layers of Level C in the section exposed by Jelinek, when viewed from a distance, are up to 8 m (Figure 19). In contrast, when viewed at close range each layer is composed of several

sub-layers and lenses that are generally less than about 50 cm in length, and often truncated (Figure 20).

These interpretations from earlier studies of Levels B and C in Tabun Cave thus present some very interesting and somewhat contradictory scenarios for the modes of occupation of the cave. While Garrod and Bate (1937) interpreted both levels as indicative of a domestic occupational site, Jelinek et al. (1973) proposed that when Level B was deposited, the cave was used as a game trap. And for Level C they proposed that the presence of ash layers was due to the burning of natural vegetation in the cave.

Our study focused on Level B and Level C, and addressed the question of how the cave was occupied during the Mousterian period in these two levels. For this purpose we determined whether or not the phytoliths in the sediments were derived from the ash of trees.

B) Results

Twelve samples from Levels B and C, both belonging to the late Mousterian, were analyzed for phytoliths as well as for the major mineral components. Four control samples from outside the cave were also studied. Table 13 lists the sediment samples analyzed for their major mineral components and phytolith concentrations. The locations of the samples were shown in figure 2.

Clay and quartz are the major mineral components of the Level B samples, as well as the brown colored samples in Level C. The latter also contain small amounts of carbonated apatite. The major component of the white Level C samples is carbonated apatite, together with appreciable quantities of clay and quartz (Table 13). Thus color is only a rough guide to major mineral composition. The origin of the carbonated apatite could be wood ash. Wood ash is composed mainly of calcite (Humphreys, Hunt & Buchanan, 1987). This calcite readily dissolves and reprecipitates as carbonated apatite due to reaction with phosphate-rich ground water common in caves (Schiegl et al.,

1996). The Level C carbonated apatite could also conceivably be due, in part, to a calcite-rich loess that has reacted with phosphate.

The yields of the inorganic acid insoluble fraction (AIF) are also listed in Table 13. The AIF is obtained after eliminating the carbonates, phosphates and organic material, which is the fraction most affected by diagenesis in this area (Weiner et al., 1995). We therefore normalized the number of phytoliths obtained during the analyses of the samples to a unit weight (1 g) of inorganic Acid Insoluble Fraction (AIF) to compare results from localities within the archaeological site that are in varying diagenetic states of preservation and to the samples from the reference collection. We also assume that the phytoliths have not, in part, dissolved. In this study we did not observe evidence of partial dissolution, except possibly in the 50 cm or so above the base of level B.

	Sample No.	Color	Depth (below datum; meters)	Major Mineral Components[3]	Acid and H_2O_2 Insoluble Fraction (weight %) (AIF)	No. phytoliths per gram acid insoluble fraction	Ratio of variable to consistent phytolith morphological forms[4]
LEVEL B	100	Brown	0.18	Cl, Q	75(55)[2]	8,000	0.9 (104)
	101a[1]	Brown	0.20	Cl, Q, Ap	88	42,000	20.8 (197)
	101b	Brown	0.20	Cl, Q, Ap	83	19,000	n.d
	101c	Brown	0.20	Cl, Q, Ap	76	33,000	n.d.
	102	Brown	0.50	Cl, Q	71	24,000	n.d.
	103	Brown	0.55	Cl,Q, Ap	76	9,000	8.2 (95)
	104	Brown	0.70	Cl, Q	83	24,000	n.d.
	105	Brown	0.70	Cl, Q	82	36,000	1.8 (103)
							average ratio: **7.93**
LEVEL C	106	Black/Brown	0.97	Cl, Q, Ap, Org	52	8,000	n.d.
	107	White	1.05	Ap, Q, Cl	32	190,000	3.6 (117)
	108	White	1.33	Ap, Q, Cl	22(23)[2]	450,000	2.7 (187)
	109	Brown	1.52	Cl, Q, Ap	67	12,000	3.0 (68)
	110	White	1.60	Ap, Q, Cl	21	420,000	2.2 (109)
	111	White	1.68	Ap, Q, Cl	9(8)[2]	140,000	2.4 (113)
	112a[1]	Brown	1.80	Cl, Q, Ap	64	18,000	1.6 (101)
	112b	Brown	1.80	Cl, Q, Ap	74	22,000	n.d.
	113	Brick red	2.00	Cl, Q, Ap	44	61,000	2.7 (131)
	114	White	2.09	Ap, CL	26	360,000	13.0 (99)
	115	Grey/Black	2.40	Cl, Ap	38	130,000	n.d.
	116	Yellow	2.50	M, Cl, Q	??	21,000	n.d.
							average ratio: **3.90**
ABOVE CAVE	117	Brown	-	Cl, Q	69	25,000	1.6 (196)
	118a[1]	Brown		Cl, Q	76	35,000	0.8 (150)
	118b	Brown		Cl, Q	83	30,000	n.d.
	119a	Brown		Cl, Q	65	13,000	n.d.
	119b	Brown		Cl,Q	80	8,000	1.6 (205)
	120	Brown		CL,Q	65	14,000	1.3 (218)
							average ratio: **1.33**

NOTES
1. Replicate analyses of the same sample.
2. Replicate analyses
3. Letters designate minerals as follows: Cl - clay; Q - quartz; Ap - carbonated apatite (dahllite); M - montgomeryte. Listed in order of decreasing abundance based on infrared spectra.
4. Number of phytoliths counted for this measurement listed in parentheses.

n.d Not determined

Table 13 – Tabun Levels B and C. Characteristics of the sediment samples studied.

The brown colored samples from Level C clearly contain more AIF than the white colored samples, reflecting mainly the higher amount of carbonated apatite contents in these brown samples. The concentrations of phytoliths in 1g of the AIF fractions are also listed in Table 13 and are plotted against the yields of AIF in Figure 22. There is an inverse relation between the two parameters for samples in which the phytolith concentrations are above 50,000 phytoliths per gram AIF. The reproducibility of the method is not sufficient to interpret variations in phytolith concentrations below 50,000 per gram AIF (Table 13). From figure 22 we infer that there is also a correlation between carbonated apatite content and phytolith concentration. We note that the samples from outside the cave have phytolith concentrations similar to those of the Level B samples (less than 50,000 per gram AIF) and some of the brown colored sediments of Level C. Figure 22 also shows the range of phytolith concentrations measured in the bark and wood, in the proportion 80:20, of trees that are now common on Mt. Carmel. These range from about 0.5 to 8.7 million phytoliths per gram AIF of the ash produced after burning the sample.

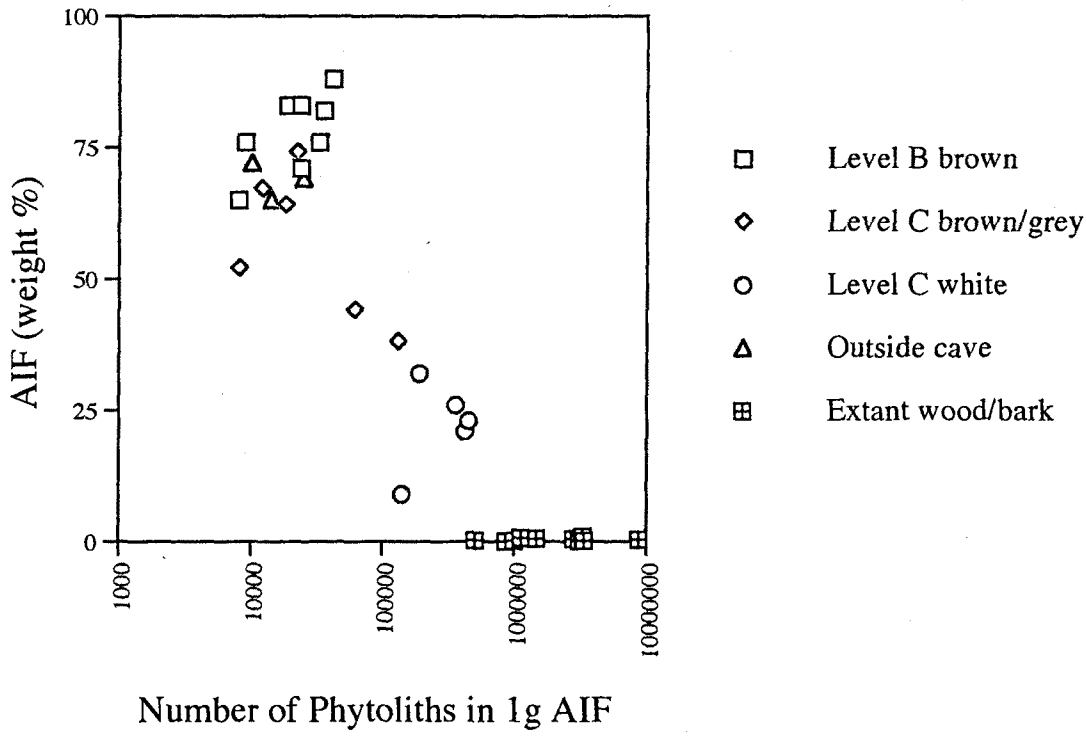

Figure 22 - Weight % acid insoluble fraction (AIF) against the number of phytoliths in the AIF fraction for Levels B and C sediments from Tabun cave, as well as sediments from outside the cave. For comparison, the numbers of phytoliths in extant wood and bark (combined in 80:20 proportions) are also shown.

The simplest explanation of these observations is that the Level C samples contain varying amounts of ash from burned trees together with clay and quartz from terra rossa soil; an explanation consistent with the macro-and micromorphological observations of Tsatskin in Albert et al. (1999a). His results showed that layers from Level C are mixtures of terra rossa soil and ash, with the white layers containing more ash than terra rossa whereas the brown and black layers are composed mainly of disrupted aggregates of terra rossa soil, usually found together with phosphatized material (possibly ash) and charcoal (Albert et al., 1999a). Tsatskin also identified a few charcoal remains. Wood charcoal is a key micromorphological indicator of burning in archaeologically related sediments (Goldberg, Lev-Yadun, Bar-Yosef, 1994). It is most abundant in the black colored layers of Level C. The white layers of Level C are composed of phosphatized fine-grained ash sediment with charcoal fragments and terra rossa. Calcite crystals with the elongate forms of calcium oxalate crystals characteristic of trees (Franceschi & Horner, 1980) were also identified by Tsatskin (Albert et al., 1999a).

We also examined the phytolith types present in the samples in order to determine whether or not they are, for the most part, derived from trees. These phytoliths were then compared to those present in the reference collection. Tables 14 a-c lists the phytoliths identified in the archaeological samples from Tabun. A first indication that the phytoliths in at least some of the samples from Levels B and C derive mainly from the ash of trees is the variation in the ratio of phytolith types with variable morphologies and consistent morphologies (v/c) in the different samples (Table 13). The average ratio is 7.93 for Tabun B and 3.90 for Tabun C (Table 13). In weighed samples of wood (80%) and bark (20%) of extant trees this v/c ratio is on the average 4.97 (Table 3). The average v/c ratios for grasses is 0.09 (Table 3). As the cave sediment samples are all well above the ratios for grasses (and leaves from the same trees, with an average ratio of 0.22) (Table 3), we inferred that they contain a significant proportion of phytoliths from wood and bark. This includes Level B samples, even though they contain relatively small amounts of phytoliths per gram AIF. This results are consistent with the micromorphology results of Tsatskin that show that sediments from Level B are composed mainly of terra rossa soil, mixed with a small amount of a wood ash component (Albert et al., 1999a).

TABUN B								
Name (See Table13 for description)	*TBS100*		*TBS101*		*TBS103*		*TBS 105*	
Consistent morphology	*Sum*	*%*	*Sum*	*%*	*Sum*	*%*	*Sum*	*%*
E s	2	-	1	-			12	-
LC e	12	-						
P Bk	15	-	3	-			11	-
P El p	1	-			1	-		
P El v							2	-
PL	4	-	4	-	8	-	5	-
Sp s			1	-	1	-	2	-
Total	**34**		**9**		**10**		**32**	
Name	*TBS100*		*TBS101*		*TBS103*		*TBS 105*	
variable morphology	*Sum*	*%*	*Sum*	*%*	*Sum*	*%*	*Sum*	*%*
I p	19	-	64	34.2	36	43.9	8	14.0
I s	6	-	100	53.5	22	26.8	44	77.2
WM	7	-	23	12.3	24	29.3	5	8.8
Total	**32**		**187**	**100**	**82**	**100**	**57**	**100**

Table 14a - Tabun cave. Phytolith morphological results from Level B.

TABUN C																
Name (See Table 13 for description)	TBS 107		TBS 108		TBS 109		TBS 110		TBS 111		TBS 112		TBS 113		TBS 114	
Consistent morphology	Sum	%	Sum	%	Sum	%	Sum	%	Sum	%	Sum	%	Sum	%	Sum	%
C p					1	-										
E p									2	6.5			1	-	4	-
E s	15	-	31	-	11	-	17	-	24	77.4	7	-	19	-	2	-
EA H											1	-				
F			2	-			1	-								
LC p					1	-	2	-			1	-				
P Bk	4	-	4	-	1	-	1	-	1	3.2	9	-	3	-		
P El p			1	-			4	-								
PL	1	-			1	-			1	3.2	19	-	7	-	1	-
ShC			1	-	1	-					1	-				
Sp s	5	-	4	-			5	-			1	-	5	-		
Sp v									3	9.7						
Total	25		43		16		30		94	100	39		35		3	-
Name	TBS 107		TBS 108		TBS 109		TBS 110		TBS 111		TBS 112		TBS 113		TBS 114	
Variable morphology	Sum	%	Sum	%	Sum	%	Sum	%	Sum	%	Sum	%	Sum	%	Sum	%
I p	27	30.3	51	43.6	19	38.8	22	33.3	24	32.0	25	41.0	27	28.1	5	5.5
I s	52	58.4	57	48.7	26	53.1	42	63.6	28	37.3	20	32.8	55	57.3	24	26.4
WM	10	11.2	9	7.7	4	8.2	2	3.0	23	30.7	16	26.2	14	14.6	62	68.1
Total	89	100	117	100	49	100	66	100	75	100	61	100	96	100	91	100

Table 14b – Tabun cave. Phytolith morphological results from Level C.

Tabun cave								
OUTSIDE								
Name (See Table 13 for description)	*TBS 117*		*TBS 118*		*TBS 119*		*TBS 120*	
Consistent morphology	*Sum*	*%*	*Sum*	*%*	*Sum*	*%*	*Sum*	*%*
B					1	1.3		
C p	15	19.7	5	6.0	9	11.7	5	5.6
C v	1	1.3	3	3.6	4	5.2	4	4.5
E s	5	6.6	5	6.0	15	19.5	27	30.3
EA PR			3	3.6	2	2.6	2	2.2
LC e	4	5.3	2	2.4	3	3.9		
LC p	5	7.9	18	21.7				
LC PO	3	3.9	12	14.5	4	5.2	1	1.1
LC w			2	2.4			6	6.7
P Bk	22	28.9	8	9.6	24	31.2	25	28.1
P El p			5	6.0				
P El s	1	1.3						
P t					1	1.3		
PL	9	11.8					8	9.0
ShC	7	9.2	19	22.9	8	10.4	2	2.2
Sp s	2	2.6	1	1.2	6	7.8	5	5.6
Sp v	1	1.3						
SS LC p							1	1.1
SS Sp/E							3	3.4
SS Sp/R	1	1.3						
Total	**76**	**100**	**83**	**100**	**77**	**100**	**89**	**100**
Name	*TBS 117*		*TBS 118*		*TBS 119*		*TBS 120*	
Variable morphology	*Sum*	*%*	*Sum*	*%*	*Sum*	*%*	*Sum*	*%*
I p	52	44.1	22	33.8	59	49.2	36	30.3
I s	34	28.8	19	29.2	24	20.0	33	27.7
IN			3	4.6				
WM	32	27.1	21	32.3	37	30.8	50	42.0
Total	***118***	***100***	***65***	***100***	***120***	***100***	***119***	***100***

Table 14c - Tabun cave. Phytolith morphological results from outside samples.

Not much can be concluded about the specific manner in which the ash accumulated (dumping, raking or accumulation in situ), because the original ash calcite transformed completely into carbonated apatite (Albert et al., 1999a). We also noted that the control soil sediments from outside the cave have v/c ratios that range from 0.8 to 1.7. They too may well contain a significant wood/bark component, because of the presence of a substantial amount of variable morphology phytoliths.

When analyzing the phytoliths with consistent morphology, the first problem is the low amount of phytoliths recovered from both levels B and C. The number is too low for a reliable interpretation of the results. Taking this fact into account, we decided to compare the forms recovered with those from some of the trees from the reference collection. It was observed that almost no phytoliths characteristic morphologies of grasses or leaves of trees were identified in the samples from both levels. Nevertheless, grass phytoliths were identified in the samples from outside the cave, which is consistent with the lower ratio obtained. Figure 23 shows some of the phytolith types identified in the Tabun samples. Phytoliths from the outside samples contain phytolith types not present in the cave.

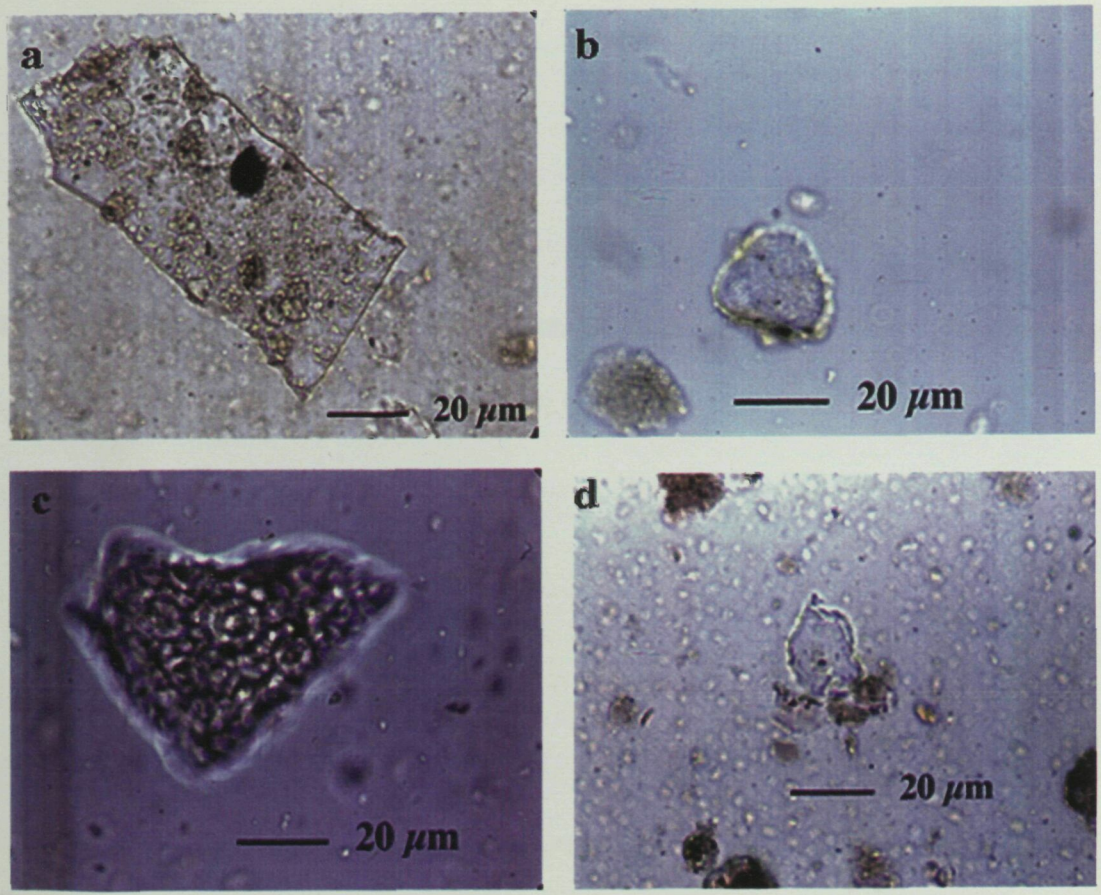

Figure 23 - Photomicrographs of phytoliths identified in Tabun cave. Pictures taken at 400x. a) Platelet from sample TB-112, Level C. b) Ellipsoid with scabrate surface identified in sample TB-105, Level B. c) Silica skeleton spheroid with rings from sample 117 (outside). d) Irregular psilate identified in sample TB-112, Level C.

Furthermore, most of the phytoliths identified in Levels B and C showed the same morphological traits. When we compared these results with the reference collection (Table 15) we noted that most, but not all, the phytoliths present in the cave sediments are present in the wood and bark of oak, in particular *Quercus calliprinos* (Kermes oak which is evergreen). There is one phytolith type that is present in oak but is absent in the sediments, namely the spheroid psilate type. This type is also abundant in many of the other trees examined to date, and is conspicuously absent in the cave sediments (Table 15). We can only surmise that for unknown reasons, these phytoliths are prone to diagenetic alteration and/or breakdown. Compared to the other trees from the reference collection, *Quercus calliprinos* (Kermes oak) has relatively large amounts of AIF and high concentrations of phytoliths per gram AIF (3.3 million compared to the average of 2.3) (Table 2). It is thus not unexpected that phytoliths of this species of oak should be well represented in the ash fraction of the sediments. The presence of oak is consistent with the palynological results obtained by Horowitz (Jelinek et al., 1973), where he identified the presence of oak in most of the samples from Level C, although in lesser amounts than in the lower layers of Tabun.

TABUN CAVE				
Phytolith types identified	*Level B (n=4)*	*Level C (n=8)*	*Outside (n=4)*	*Extant trees containing the phytoliths types observed in wood/bark fraction.*
Platelet	4	6	2	*Quercus calliprinos *, Crataegus aronia **
Ellipsoid scabrate	3	8	4	*Quercus calliprinos , Pistacia palaestina ***
Parallelepiped blocky	3	7	4	*Quercus ithaburensis**, Ceratonia siliqua **, Olea europaea **, Amygdalus communis **, Crataegus aronia*
				*Styrax officinalis ***
Spheroid scabrate	3	5	4	
Parallelepiped elongate psilate	2	2	1	*Quercus calliprinos **, Ceratonia siliqua **, Pistacia palaestina ***
Long cell echinate	1	0	3	
Parallelepiped elongate verrucate	1	0	0	
Long cell wavy	0	0	2	
Short cell	0	3	4	*Quercus calliprinos **, Quercus ithaburensis **, Ceratonia siliqua **, Cupresus sempervirens ***
				*Amygdalus communis **, Styrax officinalis **, Crataegus aronia ***
Long cells psilate	0	3	2	*Quercus calliprinos **, Cupressus sempervirens ***
Ellipsoid psilate	0	3	0	*Quercus calliprinos *, Quercus ithaburensis *, Ceratonia siliqua **, Pistacia palaestina *, Pinus halepensis*
				Olea europaea
Fibre	0	2	0	
Cylindroid psilate	0	1	4	*Quercus calliprinos *, Ceratonia siliqua **, Amygdalus communis **, Crataegus aronia ***
Spheroid verrucated	0	1	1	
Epidermal appendage. Hair	0	1	0	*Quercus calliprinos **
Long cell polylobate	0	0	4	
Cylindroid verrucate	0	0	4	
Epidermal appendage. Prickle	0	0	3	
Silica skeleton spheroid/ellipsoid	0	0	2	
Bulliform	0	0	1	
Silica skeleton long cells psilate	0	0	1	
Parallelepiped thin	0	0	1	*Styrax officinalis **
Spheroid psilate	0	0	0	*Quercus ithaburensis , Ceratonia siliqua **, Pistacia palaestina , Pinus halepensis*
** Phytoliths identified only in wood in more than 5%*				
*** Phytoliths identified only in bark. Phytoliths that were present in less than 10% of the total counted were not added here due to the possibility of contamination.*				

Table 15 - Phytoliths identified in Levels B, C and outside from Tabun cave in comparison to the phytoliths observed in wood and bark of the plant reference collection. The number of samples containing phytolith types is in brackets.

C) Discussion

The results show that phytoliths in Level B and Level C from Tabun cave derived almost entirely from wood and bark, and not from grasses, based on the preponderance of phytoliths with variable morphology as compared to those with consistent morphology. Even those phytoliths with consistent morphology were characteristic of wood/bark of local trees, while grasses were practically absent. However the results of the phytoliths with consistent morphology should be taken cautiously due to the low amount of phytoliths of these type recovered. These results are, therefore, more consistent with a domestic occupation activity, mainly in Level C, than from the burning of natural vegetation in the cave. This does not support Jelinek et al.'s (1973) suggestion that the source of the ash was the periodic burning of vegetation that had grown in the cave. This view of Level C is more consistent with the interpretation of Garrod and Bate (1937). It does support Garrod and Bate's (1937) interpretation that the mode of occupation during this period was as a domestic occupation site. One curious observation is that we did not observe grass phytoliths in the Levels B and C sediments,

even though they are present today in the terra rossa above the cave. Grass may not have grown in the immediate area around the chimney at that time, because the area was forested. However it should be taken into account the low number of phytoliths with consistent morphology noted in these samples which produce a big error margin.

The mode of occupation during the Tabun B period could also be interpreted as domestic, albeit probably ephemerally during both winter and summer, based on the cementum study (Lieberman, 1993). The opening up of the chimney must certainly have influenced the mode of occupation, particularly towards the rear of the cave. The presence of a higher proportion of finished implements and whole limb bones in the Level B sediments (Garrod & Bate, 1937) as compared to the older layers also implies a somewhat different mode of occupation. Jelinek et al. (1973) inferred from these observations that the cave was used mainly as a butchering site. Our results show that if this was indeed so, fires were also lit during this period even though there were no visible ash layers. The relatively small proportion of ash in the sediments from Level B does not imply that the intensity of occupation was low, as the ash was most likely diluted by a high rate of sedimentation of soil through the chimney. Garrod and Bate (1937) did observe the presence of a few hearths in the level B sediments.

The resemblance of the brown sediments to the regional soil type in both levels was confirmed by the macro and micromorphological analyses carried out by Tsatskin (Albert et al., 1999a). His results showed that Level B and Level C are composed mainly of terra rossa soil and ash from wood/bark mixed in varying proportions. The ash component of Level B sediments is very low. In Level C there are highly variable proportions of ash and terra rossa, that usually correspond to the white layers being rich in ash, and the others rich in terra rossa. The color variations do not however reflect the fact that in some white layers considerable amounts of terra rossa are present and vice-versa (Tsatskin in Albert et al., 1999a). The sediments were, most probably, deposited in the cave through the chimney, which opened at the beginning of Tabun C and increased considerably in size during the Tabun B period.

The simplest way to interpret these observations would be to envisage a more or less consistent mode of occupation of the cave through both Tabun B and C periods, that resulted in the deposition of bones, tools and ash. However due to the opening and

enlarging of the chimney, the rate of sedimentation varied sporadically during Tabun C and increased dramatically during Tabun B. Thus the ash that was more or less continuously produced was diluted to differing extents by the influx through the chimney of terra rossa soil.

5.3 – Results of phytolith analyses of Middle and Upper Paleolithic levels of Kebara cave

A) Introduction:

Kebara cave is one of the most intensively studied prehistoric caves in the Old World. The accumulated body of knowledge includes detailed information on the sediments, the stratigraphy, the lithics, animal bones and wood charcoal as well as the two Neanderthal skeletons found in the cave (Bar-Yosef et al., 1992). The cave also contains a large number of preserved hearths, visible to the naked eye. All these factors thus make Kebara cave a unique location to investigate the phytoliths in the sediments in relation to the use of fire by humans, as well as issues of phytolith preservation.

Kebara cave is located on the western face of Mt. Carmel (northern Israel), about 30 km south of Haifa and 13 km south of Tabun cave in Wadi el-Mughara (Nahal Ha-Me'arot) (Figure 1). It is 2.5 km east of the present Mediterranean shoreline and about 60 m above sea level (Israel Reference Grid 1442/2182). Kebara cave formed in

Cretaceous dolomite (Bar-Yosef et al., 1992). The entrance has an arched shape, and faces north-northwest. (Figure 24). The cave dimensions are about 26 x 20 m, and consists of one large chamber that opens westwards to the sea (Figure 25). The chamber contains three vaults and a small chimney at the rear of the cave (Goldberg & Laville, 1989; Laville & Goldberg, 1989).

The coastal plain in front of the cave is composed of calcareous sandstone ridges (kurkar) (Laville & Goldberg, 1989), on an elongated alluvial plain (Farrand, 1979 in Bar-Yosef et al., 1992). The present arboreal vegetation consists mainly of carob *(Ceratonia siliqua)* and lentisk *(Pistacia lentiscus)*, which are characteristic of open forest, mainly on the coast. The hills are dominated by two different types of vegetation, the evergreen oak or Kermes oak *(Quercus calliprinos)* on the northern slopes, and the deciduous oak or Tabor oak *(Quercus ithaburensis)* on the southern slopes (Baruch, Werker & Bar-Yosef, 1992). The type of soil common in the area is terra rossa, which is composed mainly of reddish-brown clay. The climate is typically Mediterranean, with mild rainy winters and hot, arid summers. Precipitation is about 550 mm per year. Mean annual temperatures are around 18°C (Baruch, Werker & Bar-Yosef, 1992).

Figure 24 - Photograph of the entrance of Kebara cave with the arched shape and facing north-northwest.

Figure 25 - Photograph Kebara cave. Chamber inside.

Stekelis made the first sounding in Kebara cave in 1927 and the first excavation was conducted in 1931 by Turville-Petre. He excavated most of the surface sediments of the cave. Five layers are defined (from A - E), which cover the periods from the Bronze Age to the Mousterian (Bar-Yosef et al., 1992). Stekelis excavated the central portion of the cave between 1951 and 1965. He exposed a series of Mousterian and Upper Paleolithic layers and hearths. The skeletal remains of a Neanderthal baby (8-9 months old) were found close to the north wall (Bar-Yosef et al., 1992). A third excavation was carried out from 1982 to 1990 by a multidisciplinary Israeli-French team (Bar-Yosef et al., 1992). The relevant results of which are described below.

Goldberg and Laville (1989, 1991) divided the stratigraphic sequence in three sections/profiles: West, South and East. The west profile includes the northern sector, the west section and the deep sounding. The total thickness of the west profile, the focus of our study, is about 8 m where the Mousterian sequence was sub-divided into 12 different units (Bar-Yosef et al., 1992).

Units XVI to XIV, above the bedrock in the deep sounding, are archaeologically sterile (Bar-Yosef et al., 1992). Unit XIII is 80 cm thick. It contains numerous hearths and a few lithic materials (Goldberg & Laville, 1989, 1991; Bar-Yosef et al., 1992). Units XII to VII, about 5 m thick, are relatively homogeneous, and seem to have accumulated quite rapidly. They are composed of numerous superimposed hearths that are *in situ*, and are separated by soft, organic-rich silt (Goldberg & Laville, 1989, 1991; Bar-Yosef et al., 1992). In Unit XII, an almost complete burial of a Neanderthal adult male was discovered in 1983 (Arensburg et al., 1985; Bar-Yosef et al., 1986; 1992). Meignen and Bar-Yosef (1988) suggest that the lithic assemblages from units XII-VII are similar to the "Tabun B-type" industry. Unit VI shows disturbances produced by geological and biological activity (Goldberg & Laville, 1989; 1991). Unit V contains a lithic industry mainly from the Mousterian period, although intrusive elements from the Upper Paleolithic industry were also recovered (Goldberg & Laville, 1989; Laville & Goldberg, 1989; Bar-Yosef et al., 1992).

Thermoluminescence (TL) dating of burnt flints from this profile, produced a sequence of ages from 48,300±3500 years B.P. for level VI to 59,900±3,500 years B.P. for level XII (Valladas et al., 1987; Valladas & Joron, 1989). These dates support the

suggestion that layers XII to VII accumulated rapidly as a result of frequent occupation (Valladas et al., 1987). Level X was also dated by electron spin resonance (ESR) using mainly gazelle tooth enamel to 60,000±6,000 years B.P. using the early uranium uptake model, and to 64,000±4,000 years B.P. using the linear uranium uptake model (Schwarcz et al., 1989).

The south profile is, in general, the partial continuation of the layers of the west profile. Unit V is the continuation of Unit VI in the west profile. It contains Middle Paleolithic elements especially at the base of the unit. Unit IV contains an as yet unidentified industry. Units I-III belong to the Upper Paleolithic period (Bar-Yosef et al., 1992). Units I to V were dated by radiocarbon giving a range from 42,000±1,800 to 46,000 years B.P. in levels IV and V respectively to 28,700±450 years B.P. for levels I-IV (Bar-Yosef et al., 1992; Bar-Yosef et al., 1996). The Epi-Paleolithic layers were completely removed by Turville-Petre.

The east profile was not systematically excavated although the cleaning of the sections shows that it resembles the units of the south profile (Bar-Yosef et al., 1992).

The sediments deposited in Kebara cave are of aeolian, colluvial, biologic and/or anthropogenic origin. Clay-rich sediments (terra rossa) are present at the entrance of the cave, together with quartz silt and sand (Bar-Yosef et al., 1992). Sediments of biological or anthropological origin are very common, as are ash layers, especially in the west profile. Note too the effects on sedimentation produced by bone accumulations, mainly in the northern wall, and other biological activities such as burrowing or digging. This is especially evident in Unit VII of the west profile. Karstic activity has also influenced the formation of the sediments in the cave (Bar-Yosef et al., 1992). The ash layers from Units XIII to VII show no signs of erosion, which indicates a stable regime of sedimentation with minimal water deposition. At the end of the Mousterian period (Unit VI) there is an increase of karstic activity with wetter conditions, as indicated by the presence of tilting and slumping (Bar-Yosef et al., 1992). This phenomenon continues into the Upper Paleolithic period. The increase in wetter conditions could be due, either to a climate change (around 40,000 years ago) or to a local change in the cave configuration. The latter could have been produced by the collapse of the face of the cliff above the entrance that made the cave more sensitive to external environmental activities, such as rainfall and runoff (Bar-Yosef et al., 1992).

The hearths in Kebara cave are mostly concentrated in the central area of the cave, and are less abundant along the northern wall. In the deep sounding, they are superimposed for more than 4 m (Meignen, Bar-Yosef & Goldberg, 1989) (Figure 26). Individual hearths are often structured with the white, gray, orange or yellow portions mostly in the upper part, and the dark brown and black layers at the base (Schiegl et al., 1996). The cave, during this period, appears to have been used continuously at least, in the central and northern areas (Meignen, Bar-Yosef & Goldberg, 1989).

The hearths have been divided into two types. The most common are flat lenses (8-10 cm thick), and are rounded or oval shaped in planar section (about 40-60 cm in diameter). The second less common group is bowl- shaped in section. They are about 10 cm thick and about 30-90 cm in diameter (Meignen, Bar-Yosef & Goldberg, 1989). A few unusual large hearths have diameters of more than 1 m and are around 30 cm thick. They probably reflect the accumulation of successive fires in the same depression. Two phases of hearth formation were observed in Units XII-VII. The rounded or oval hearths correspond mainly to in situ fireplaces, but in some cases, the ashes were spread over a wider area, creating an irregular shape of white ashes (Bar-Yosef et al., 1992; Goldberg & Bar-Yosef, 1998).

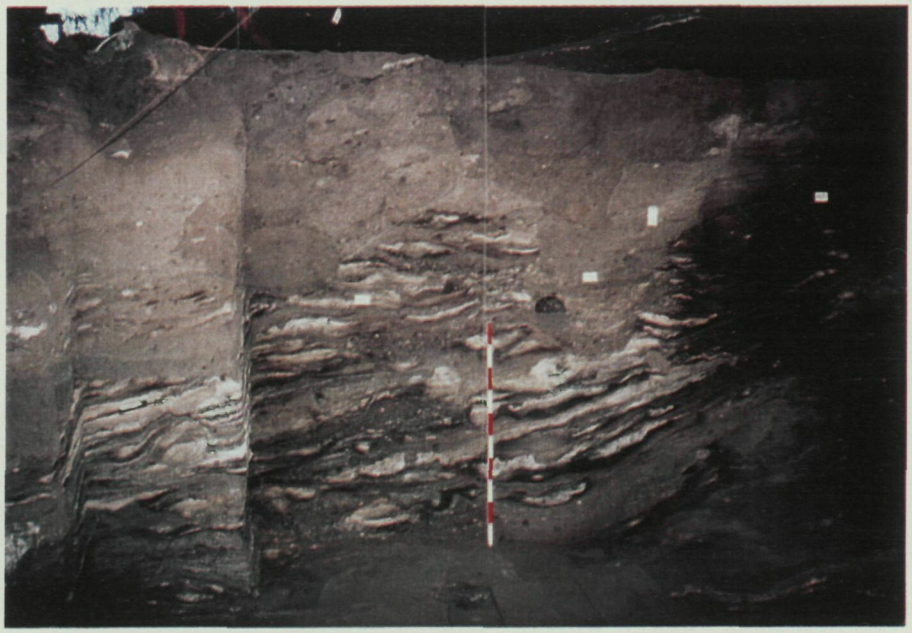

Figure 26 – Photograph of Kebara cave. Section from the deep sounding with the superimposed hearths *in situ* showing different coloration. Scale bar: 10 cm intervals.

Schiegl et al. (1994, 1996) analyzed 86 hearths from different areas of Kebara cave, as well as the underlying sediments, and the sediments that separate the hearths. The results obtained showed that 7 hearths were mineralogically well preserved as indicated by the presence of calcite, 46 were composed of a variety of phosphate minerals and 33 were mainly siliceous aggregates (Schiegl et al., 1996). Siliceous aggregates are a minor component (about 2 weight and volume percent) of fresh ash. One of the striking results is that siliceous aggregates were often present not only in the hearths, but also in the sediments immediately underlying the hearths, as well as those separating the hearths. Furthermore there are whole areas in Kebara cave where there are almost no hearths and where siliceous aggregates are an important component of the sediments. Micromorphological analyses of the hearths carried out by P. Goldberg (Bar-Yosef et al., 1992, Meignen, Bar-Yosef & Goldberg, 1989) showed the presence of phytoliths, including grass phytoliths. Goldberg & Bar-Yosef (1998) also concluded that the ashy deposits located toward the rear of the cave are composed of thick accumulations of ash as a result of Middle Paleolithic dumping activities.

Schiegl et al. (1994, 1996) established the relationship between the "siliceous aggregates" from fresh cut trees and the material identified in archaeological samples from Hayonim and Kebara caves. Schiegl et al. (1994, 1996) also showed that the hearths from Kebara cave undergo a series of diagenetic processes that do not affect equally the entire area of the cave. Calcite, the most common mineral of fresh ash, undergoes a series of dissolution and reprecipitation steps in which phosphate minerals are formed. After several such steps in which part of the minerals dissolved and are not reprecipitated, only the relatively stable component of ash, in this case, mainly siliceous aggregates and phytoliths, remain. With time the siliceous aggregates also undergo diagenesis and other precipitation products are formed (Schiegl et al., 1996). Thus under these conditions the phytoliths are probably the most durable of all ash components. Schiegl et al. (1996) also showed that during this process there is a reduction in the original sediment volume, because of compacting due to dissolution of the ash-derived minerals.

Charcoal fragments, were identified by Baruch, Werker & Bar-Yosef (1992) from Middle and Upper Paleolithic levels. Their results indicated that *Quercus ithaburensis* (Tabor oak) and *Quercus calliprinos* (Kermes oak) are the most abundant species. *Pistacia* and *Crataegus* (Hawthorn) were also identified. One fragment of *Salix* (Willow) and one of *Ulmus* (Elm) were noted. The composition of the charcoal fragment assemblage is *grosso modo*, very similar to the composition of the present vegetation in the region. Baruch, Werker & Bar-Yosef (1992) suggested that this resemblance may be due to the fact that most of the analyzed specimens originated in layers dating to the beginning of an interstadial phase (stage 3 in terms of the universal oxygen isotope stratigraphy). In this phase the climatic conditions in the Kebara area may have been similar to the present. Lev & Kislev (1993) identified charred kernels from samples from the Middle Paleolithic levels. Many were from legume seeds. They also identified grass grains, oak acorns and pistachio nuts. Most of the kernels recovered were edible. The presence of the *Leguminoseae* family, mainly wild peas, suggests that the cave was occupied during the spring, since wild peas are available in the Mount Carmel area in April and May (Lev & Kislev, 1993; Bar-Yosef et al., 1992).

Thus, the study of the archaeological remains from Kebara cave, and especially those related to the presence of the ash layers, suggests that an analysis of the phytoliths in Kebara cave could be of much interest, both in terms of understanding phytolith preservation and identifying different type of plant taxa used for fuel or for other purposes.

B) Results

Sixteen samples from Kebara cave were analyzed. These samples were collected mainly from the deep sounding, as well as several other areas of the cave. Four samples from different spots outside the cave were also analyzed for comparison. Table 16 lists the samples analyzed, together with the numbers assigned to them, locations in the cave, color, major mineral components, percentages of acid insoluble fraction (AIF), numbers of phytoliths per 1g of AIF, and the ratios between phytoliths with variable and consistent (v/c) morphologies. Figure 3 shows the locations of the samples in the excavation plan.

Area	Sample n.	Square	Color	Depth (meters below datum)	Major mineral components (1)	% AIF ($HCl+HNO_3$ and H_2O_2) (2)	# phyt.1g. AIF	Ratio v/c (3)	Notes from field observation
Deep sounding U. XV	RKE 6	M20	brown	10,38	SA, L,Q, O	31.0	6,456,000	1,9	sterile
U. XV	RKE 7	M20	brown/white spots	10,15	SA, L, M Q, O	39,2	3,918,000	2	sterile
U.XIV?	RKE 8	M20	hearth rubefacted	9,83	M Q, SA, O	13,6	2,749,000	1,3	no flint/bones
U.XIII	RKE 11	M20	white	9,73	M Q, SA, O	25,9	1,000,000	1,8	hearth?
U.XIII	RKE 18	M20	yellow	8,68	SA, M,Q	52,7	650,000	0,9	hearth
U.XIII	RKE 19	M20	brown	8,58	SA, L,Q, O	39,2	4,295,000	1,2	above hearth
U.XII	RKE 28	M20	white	7,71	SA, Q, O	89,2	13,045,000	7,1	hearth
U.XII	RKE 29	M20	black	7,76	SA, L,Q, O	56,0	10,352,000	3,5	same hearth
U.XI	RKE 30	M20	brown	7,60	SA, L, Q, O	90,6	7,671,000	0,9	above former hearth
West profile U.VIII	RKE 38	O21	white	6,10	SA, L, M, Q, O	46,7	921,000	0,5	hearth
U.VIII	RKE 39	P21	white	6,09	SA, L, M, Q, O	49,2	884,000	1,1	hearth (same as former one)
U.VII	RKE 40	P21	white	5,90	SA, M, L, Q, O	54,2	920,000	1,7	base, hearth
North-east sector	RKE 37	G13	white	6,90	C, Q, SA, O	9,9	5,426,000	18,8	hearth
North-east sector	RKE 43	I14	white	7,50	C, Q, SA, O	20,6	10,457,000	11,6	hearth
East profile U.III	RKE 44	O14	brown	5,95	SA, L, Q, O	61,9	405,000	1,4	sediment above diatom layer (P. Goldberg)
East profile U.III	RKE 45	O14	brown	5,85	SA, L, Q, O	73,6	5,738,000	1	sediment from diatom layer (P. Goldberg)
Outside	RKE 1			North of the cave	Cl, Q	57,7	82,000	1,6	Terra rossa
Outside	RKE 3			North of the cave (higher elevation)	Cl, Q	74,0	55,000	1,4	Terra rossa
Outside	RKE 32			Next to chimney	Cl, Q	61,9	71,000	0,9	Terra rossa
Outside	RKE 34			South slope	Cl, Q	70,4	23,000	1,3	Terra rossa

Table 16 – Kebara cave. Locations and descriptions of samples, as well as results of major mineral components, % of AIF, n. of phytoliths per 1 g of AIF and ratio between phytoliths with variable consistent morphologies (v/c).
1 - Key to symbols: C - calcite; Cl - clay; L - leucophosphites; M - montgomeryte; O - opal; Q - quartz; SA - siliceous aggregates. Minerals underlined belong to the major mineral components.
2.- % Acid insoluble fraction (AIF) after both acid and oxidation treatments
3.- Ratio of variable to consistent morphology phytoliths

Choice of samples

Samples RKE6 to RKE40 were selected in a single stratigraphic sequence to determine whether there are differences in phytolith composition with depth and in relation to different sediment types. This sequence extends from the bottom of the cave in the deep sounding (10.4 m below datum) to almost the top of the Mousterian (5.9 m below datum) (Table 16). The two deepest samples, RKE6 and RKE7, were from archaeologically sterile sediments (Bar-Yosef et al., 1992). Samples RKE28 and RKE29 belonged to the same hearth. The former was from the white layer and the latter from the black layer. Brown sediment from above this hearth was also analyzed (RKE30). Samples RKE38 to RKE40 were selected from a different archaeological grid square since it was not possible to follow the same stratigraphic sequence in the deep sounding. Samples RKE38 and RKE39 were from the same hearth and were located next to each other (Figure 3). Samples RKE37 and RKE43 are from the north-east sector of the cave and were selected because the major mineral component is calcite.

As fresh wood ash is also composed mainly of calcite (Humphreys, Hunt & Buchanan, 1987), these hearths, are thought to be well preserved mineralogically (Schiegl et al., 1994, 1996). Sample RKE37 was collected from square G13 (Figure 3). This ashy feature has been the subject of earlier mineralogical and micromorphological studies (Schiegl et al., 1994, 1996; Courty, Goldberg & Macphail, 1989) (Figure 27). Two samples (RKE44 & RKE45) from the Upper Paleolithic period were also analyzed for comparison. RKE45 was described by P. Goldberg (personal communication, Goldberg & Bar-Yosef, 1998) as a layer containing both diatoms and phytoliths (Figure 28). Four samples were also collected from outside the cave (Table 16). Thus the samples analyzed enabled us to address questions relating to correlations between the physical appearances of the hearths in the cave, their stratigraphic locations, and relations between mineralogy and phytolith composition.

Figure 27 - Photograph of Kebara cave. Square G13 in the northeast section of the cave corresponding to sample RKE37. Calcitic hearth. Scale bar: 10 cm intervals.

Figure 28 - Photograph of Kebara cave. Square O14 corresponding to sample RKE45 where the diatom layer was identified. Upper Paleolithic layer. Scale bar: 10 cm. Interval.

Mineralogy

Fourier transform infrared spectroscopy (FTIR) was used to identify the major mineral components of the samples (Table 17). These are predominantly the phosphate minerals, montgomeryte and leucophosphite, as well as the relatively insoluble quartz and the wood derived siliceous aggregates. In two hearths in the north of the cave (RKE37 & RKE43), calcite is the major component. The phosphate minerals are thought to be transformation products of the original calcitic component of the ash (Schiegl et al., 1996). Note that clay was not a major component of any of these samples. Analyses were carried out on the untreated samples, as well as on samples treated to remove mainly the carbonate and the phosphate minerals, as well as the organic matter. Table 17 shows that, as expected, while the major mineral components based on FTIR analysis are composed mainly of acid soluble minerals, the weight percent values of the AIF are low, and vice versa. This is consistent with the observations of Schiegl et al. (1996) who observed that most of the sediments in Kebara were dominated by the presence of ash-derived minerals.

Sample	*Square depth (m)*	*Major minerals*	*Weight % pellets*	*Major mineral components of AIF*	*SA/O*	*N. phytoliths1g AIF*
RKE6	M20	SA, L	44.4	Q	1.25	6,456,000
	x=65		13.2	SA (Q rich)		
	y=0		17.7	SA		
	z=10.38		19.3	O		
			3.5	O		
			1.6	O		
			0.3	O		
RKE7	M20	SA, L, M	24.1	Q	10.46	3,918,000
	x=65		16.7	SA (Q rich)		
	y=0		52.6	SA		
	z=10.15		5.9	O		
			0.7	O		
RKE8	M20	M (crystalline)	44.0	Q	4.78	2,749,000
	x=45		19.7	SA (Q rich)		
	y=0		26.7	SA		
	z=9.83		9.0	O		
			0.7	O		
RKE11	M20	M (crystalline)	44.5	Q	6.50	1,000,000
	x=68		10.8	Q		
	y=0		38.7	SA		
	z=9.73		4.7	O		
			1.3	O		
RKE18	M20	SA, M	42.6	Q	-	650,000
	x=90		13.3	SA (Q rich)		
	y=0		41.4	SA		
	z=8.68		2.7	SA		
RKE19	M20	SA, L	59.3	Q	2.23	4,295,000
	x=90		10.0	Q, SA		
	y=0		21.2	SA		
	z=8.58		9.5	O		
RKE28	M20	SA	23.9	Q	0.83	13,045,000
	x=90		9.9	Q		
	y=0		9.6	SA		
	z=7.71		20.3	SA		
			15.7	O		
			15.8	O		
			4.7	O		
RKE29	M20	SA, L	23.3	Q	3.57	10,352,000
	x=90		17.3	Q, SA		
	y=0		46.3	SA		
	z=7.76		10.5	O		
			1.6	O		
			0.9	O		
RKE30	M20	SA, L	29.2	Q	0.10	7,671,000
	x=90		11.5	Q		
	y=0		5.2	Q, SA		
	z=7.6		34.2	O		
			10.8	O		
			5.4	O		
			3.7	O		
RKE38	O21	SA, L, M	31.8	Q	13.35	921,000
	x=40		22.1	SA (Q rich)		
	y=0		41.3	SA		
	z=6.1		4.8	O		
RKE39	P21	SA, L, M	34.3	Q	31.13	884,000
	x=20		32.5	SA (Q rich)		
	y=50		31.1	SA		
	z=6.09		2.0	O		
RKE40	P21	SA, M, L	25.8	Q	16.21	920,000
	x=95		24.4	SA (Q rich)		
	y=55		45.6	SA		
	z=5.9		4.3	O		
RKE37	G13	C	22.5	Q , C (remnant)	1.98	5,426,000
			26.3	SA, (Q rich),		
			14.0	SA		
			11.1	SA		
			23.2	O		
			2.8	O		
RKE43	I14	C	18.4	Q	3.58	10,457,000
	x=0		9.3	SA, (Q rich)		
	y=0		26.0	SA		
	z=7.5		28.5	SA		
			12.7	O		
			5.1	O		
RKE44	O14	SA, L	44.3	Q	11.67	405,000
	x=50		23.7	Q, SA		
	y=0		29.5	SA		
	z=5.95		0.7	O		
			1.9	O		
RKE45	O14	SA, L	47.5	Q	5.07	5,738,000
	x=50		24.9	Q, SA		
	y=0		23.1	SA		
	z=5.85		4.0	O		
			0.5	O		
	Codes:					
C: Calcite; Cl: Clay; L: Leucophosphite; M: Montgomeryte; O: Opal; Q: Quartz; SA : Siliceous aggregates.						

Table 17 - Kebara cave. FTIR results showing the major mineral components, the ratio between Siliceous aggregates and opal SA/O and number of phytoliths per 1 g of AIF.

These samples were then further separated into different fractions using heavy liquids. The major components of the AIF are quartz, siliceous aggregates and opal (Table 17). Observations in the light microscope showed that the opal is composed mainly of opalline phytoliths, and in some samples it may also be formed inorganically as a result of diagenesis. The siliceous aggregates are, following Schiegl et al. (1994. 1996) assumed to be from wood. There are several possible sources of quartz, including from the soil, aeolian and the siliceous aggregates themselves, which in essence are also soil-derived. Siliceous aggregates are present in all the cave samples (Table 17). This includes the sediments that were sampled between the hearths. Ash is therefore clearly a major component of all the sediments, and not only in visible hearths. In Kebara cave, color is not a good indication of mineralogy (Table 16) (Albert et al., 1999b).

Near the northern wall of the cave, two areas still show the presence of the original ash-derived calcite. The samples corresponding to these areas are RKE37 and RKE43. Figure 29 shows the spectra obtained through the FTIR analyses for sample RKE37.

The results show the presence of calcite in the untreated sample and the presence of quartz, siliceous aggregates and opal in the treated samples.

Samples RKE8 and RKE11 show the presence of montgomeryte as a major mineral component, which according to Schiegl et al. (1996) precipitates before the formation of leucophosphite. Samples RKE7 and RKE18, which were collected immediately above and below the former two samples, also show the presence of montgomeryte as a major mineral component, although together with siliceous aggregates and leucophosphite. Micromorphological analyses carried out by P. Goldberg of sample RKE18 showed that phosphates were dissolved later. These results, therefore suggests a better mineralogical preservation at this depth of the deep sounding.

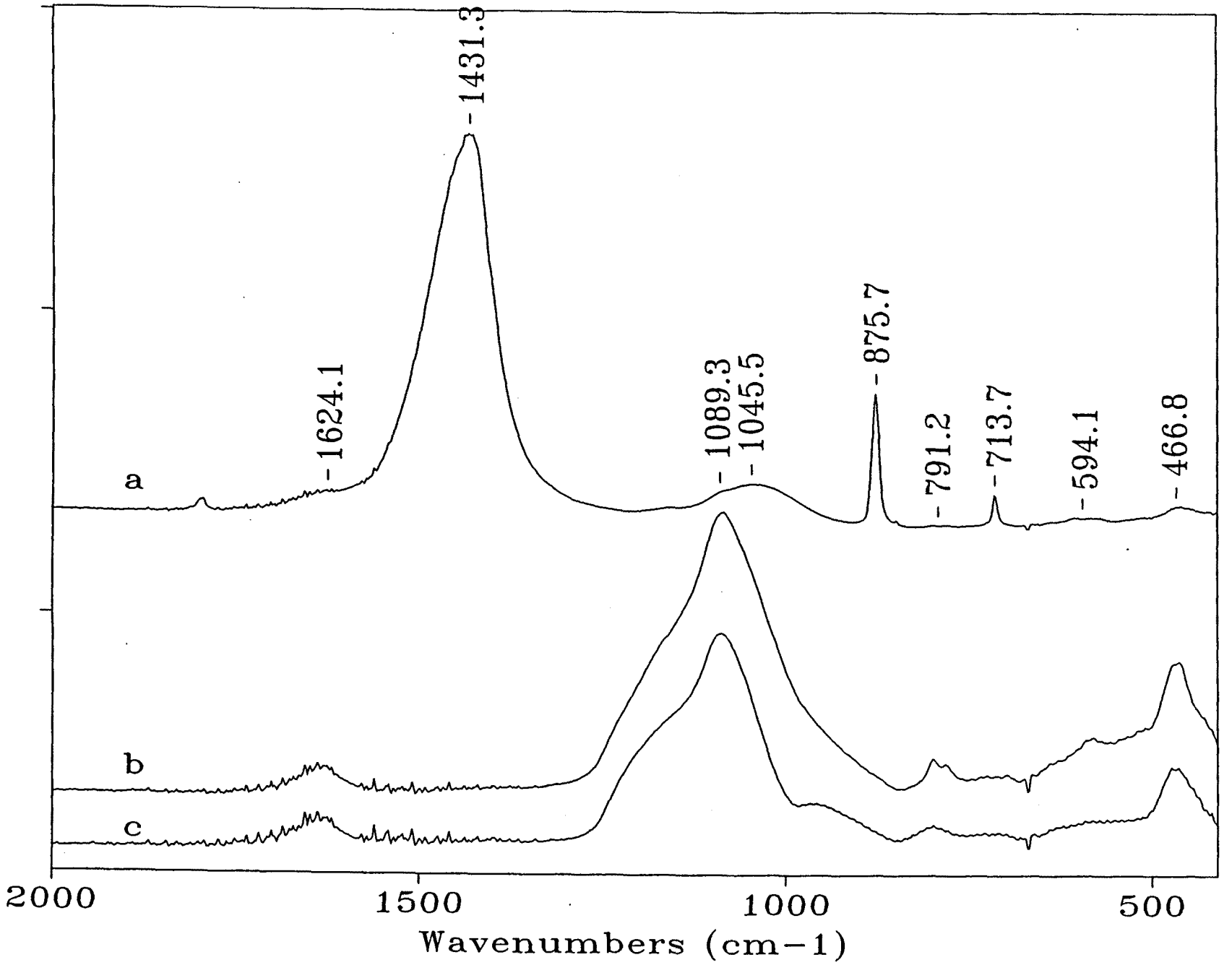

Figure 29 - FTIR spectra from Kebara cave, sample RKE37, square G13. a) Sample before acid treatment, with the highest point showing the presence of the ash-derived calcite. b) Sample after acid treatment between densities 2.4 - 2.0. c) Sample after acid treatment between densities 2.0 - 1.4. b) and c) show the presence of quartz, siliceous aggregates and opal.

FTIR results and phytolith results indicate that sample RKE28 is in a more advanced stage of dissolution, with only the more insoluble components still present: siliceous aggregates, opal and quartz, whereas all the phosphates are absent from the results (Albert et al., 1999b). Figure 30 shows the spectra with the mineralogical FTIR results from the untreated (a) as well as the treated samples (b & c). The three spectra show similar results with the pesence of siliceous aggregates, opal and quartz.

Note that clay was not a major component of any of these samples. All of the samples show a great difference in mineral composition compared to the four samples analyzed from outside, which show clay and quartz as major mineral components (Albert et al. 1999b). Figure 31 shows the FTIR spectra of one of the samples from outside (RKE3) with the results from the untreated sample (a) and the treated samples (b & c). The three samples show the major presence of Clay in Quartz present in varying proportions.

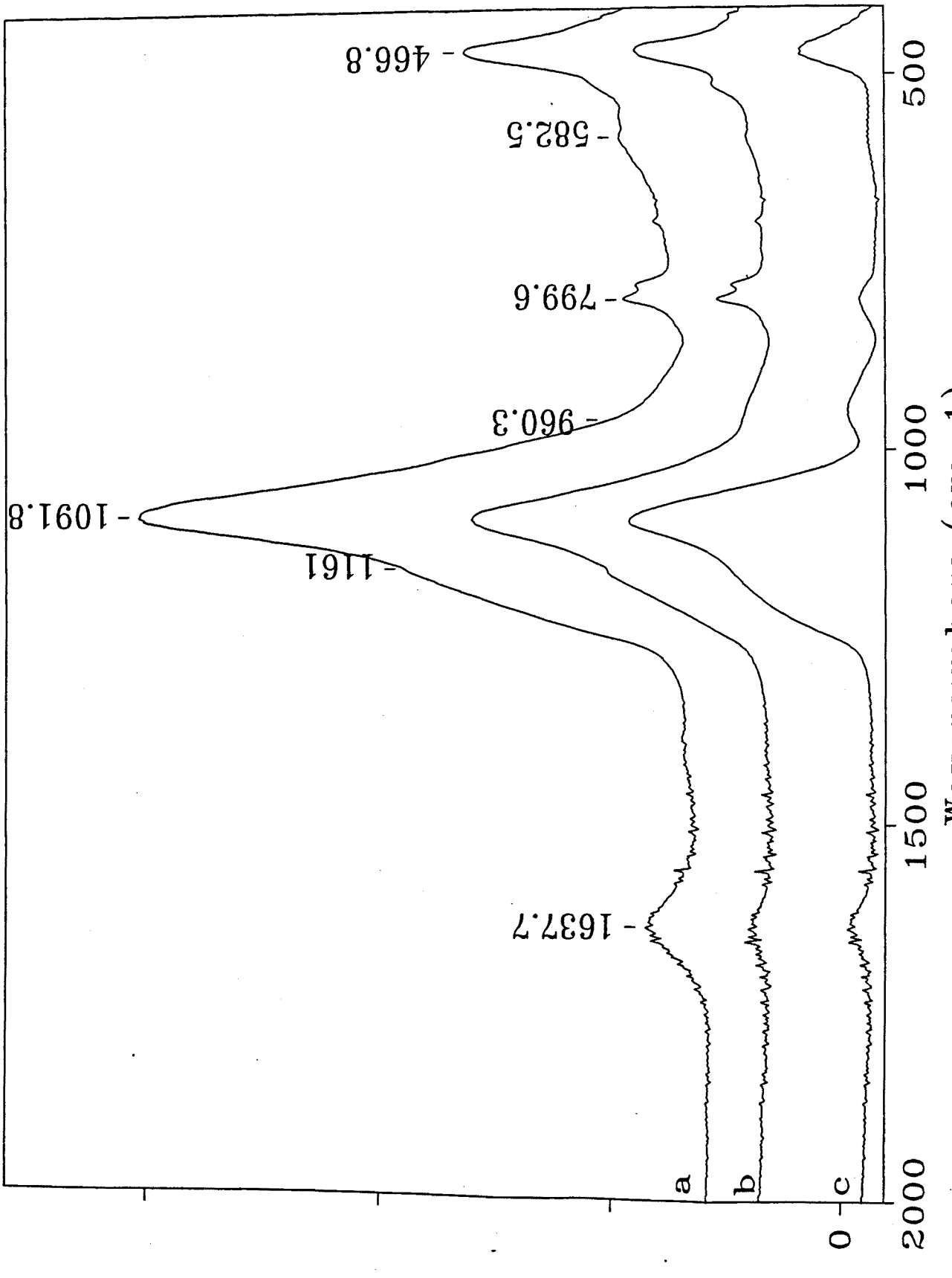

Figure 30 - FTIR spectra from Kebara cave, sample RKE28 in the deep sounding. a) Sample before acid treatment, with the highest point showing the presence of the siliceous aggregates. b) Sample after acid treatment between densities 2.4 - 2.0. c) Sample after acid treatment between densities 2.0 - 1.4 indicating the presence of pure opal.

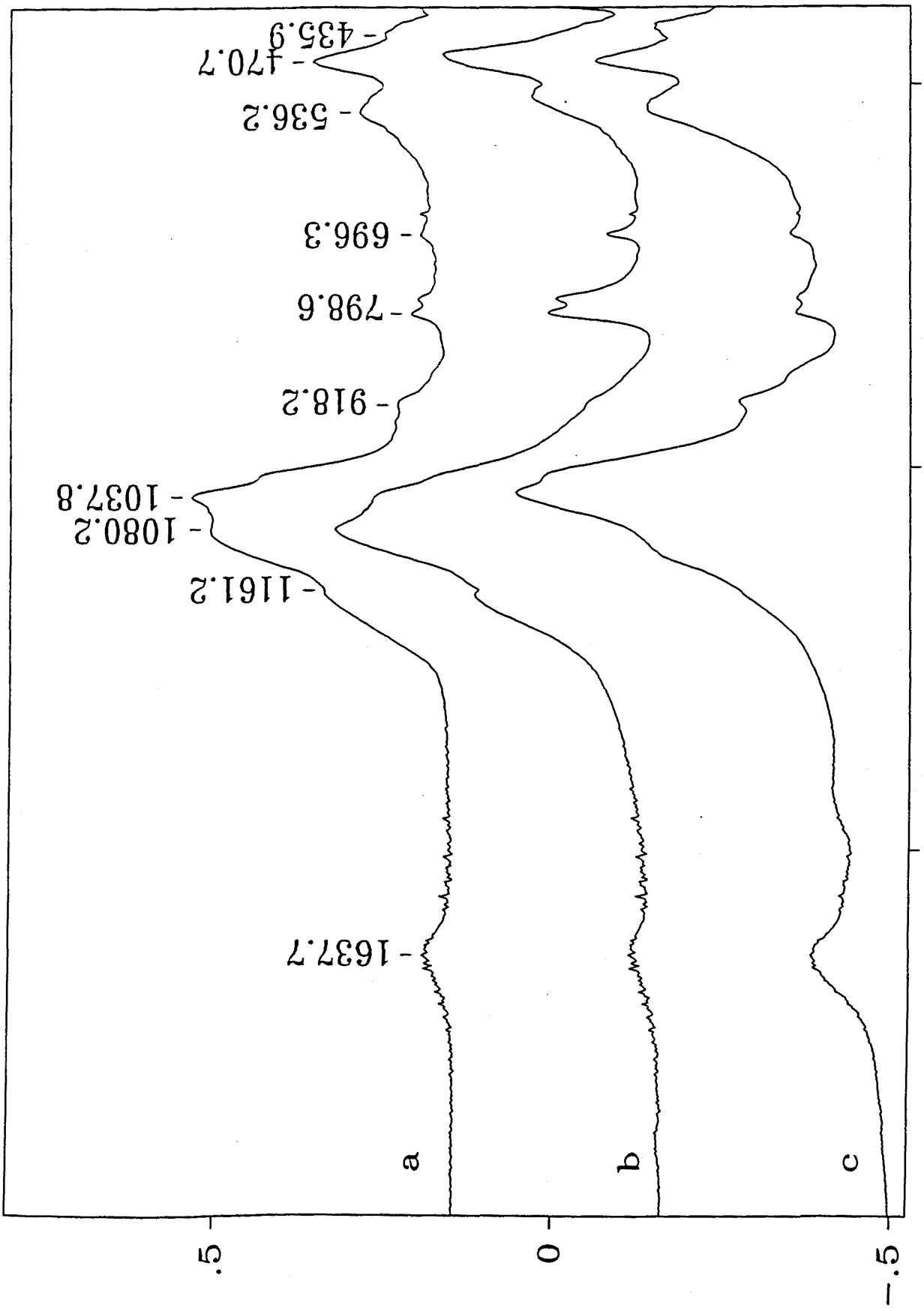

Figure 31 - FTIR spectra from Kebara cave, sample RKE3 from outside the cave. a) Sample before acid treatment, with the highest point showing the presence of clay. b) Sample after acid treatment between densities 2.4 - 2.0. c) Sample after acid treatment between densities 2.0 - 1.4.

Phytoliths

Phytoliths are present in all the samples analyzed. There are ten times as many phytoliths in the AIF fractions from cave samples as compared to the sediments outside the cave (Table 16). There is no correlation between the color of the sample or whether they were derived from a hearth, and the number of phytoliths. Two of the samples with the highest number of phytoliths (RKE28 & RKE29), belong to the same hearth (Table 16) (Albert et al. 1999b).

Any detailed analysis of the phytoliths needs to take into account possible effects of diagenesis on the preservation of the phytolith assemblages. Of all the samples analyzed, the phytoliths extracted from the two calcitic hearths (RKE37 & RKE43) are conspicuously different. They contain very few phytoliths with consistent morphology, and the v/c ratios are the highest of all the samples analyzed. Sample RKE43 did not contain enough phytoliths with consistent morphology to quantitatively study the morphological characteristics (less than 50 phytoliths with consistent morphology were

identified). According to our test reported in the reference collection section, an amount of 50 phytoliths counted with consistent morphology give an error margin of 40% (Table 4). The absolute numbers of phytoliths per gram AIF in both samples are also relatively high (Table 16). All the phytoliths show abundant signs of having been partially etched (weathered morphotypes) and many must have dissolved (Albert et al. 1999b). In figure 6c it could be observed a partially dissolved phytolith, with the formation of rounded cavities on the surface of the phytolith, which indicates dissolution due to high pH (Benayas, 1963).

In fact, signs of partial dissolution of phytoliths were noted in all the samples, but these were far less severe than those from the calcitic hearths. Only sample RKE28, and to a lesser extent RKE29, did show many weathered morphotypes, which were mainly confined, to the variable morphology types. Consistent morphology phytoliths in these samples were numerous and generally well preserved. The relatively high concentrations of opal in these two samples may also be due to partial loss of the siliceous aggregate fraction of the AIF. We therefore do not think that the phytolith analyses presented here were significantly affected by diagenesis, except for the two calcitic hearth samples, and in some respects the white and, to a lesser extent, black

layers of one of the hearths from the deep sounding (RKE28 & RKE29) (Albert et al., 1999b).

Table 16 shows the ratios of variable to consistent morphology (v/c) phytoliths in the samples. The values are all between 0.5 and 1.9, except for the diagenetically altered samples from the two calcitic hearths, and the one hearth in the deep sounding (RKE28 & RKE29), where the values are much higher. The v/c values for fresh wood and bark (80:20) in the trees analyzed for the reference collection, range from 1.25 to 17.44 with an average of 4.97 (Table 3). The values obtained in Kebara cave are therefore generally lower than those expected for wood and bark. We therefore conclude that they must contain a significant contribution of phytoliths from other plant sources. Tables 18a – 18d list the consistent morphology phytolith types identified, as well as the gross divisions of variable morphology types in all the samples analyzed from Kebara cave. In the consistent morphology group, two basic types of phytoliths are recognized: those from dicotyledons and those from monocotyledons, which in Kebara cave are mainly grasses.

KEBARA CAVE																		
Name (See Table 16 for description)	RKE 6		RKE 7		RKE8		RKE11		RKE18		RK19		RKE28		RKE29		RKE30	
Consistent morphology	Total	%	Total	%	Total	%	Total	%	Total	%	Total	%	Total	%	Total	%	Total	%
B	1	0.2			5	1.4									1	0.3		
C p	11	2.4	15	3.2	28	7.9	19	11.4	64	30.8	20	6.0	11	4.9	30	8.4	23	5.6
C p Bu			1	0.2														
C s			2	0.4	1	0.3	4	2.4	1	0.5	25	7.5					1	0.2
C v	7	1.5	14	3.0	8	2.2	3	1.8	1	0.5	94	28.2	2	0.9			14	3.4
D p																	1	0.2
E p	5	1.1	4	0.9	3	0.8			10	4.8			8	3.6	1	0.3	3	0.7
E s	21	4.5	40	8.7	17	4.8	5	3.0	8	3.8	46	13.8	4	1.8	12	3.4	17	4.1
E v					1	0.3					13	3.9						
EA H	20	4.3	8	1.7	1	0.3	1	0.6	2	1.0	1	0.3			2	0.6		
EA H Bozarth			1	0.2														
EA PA	1	0.2	3	0.6														
EA PR	12	2.6	14	3.0	17	4.8	8	4.8	8	3.8	3	0.9	14	6.3	7	2.0	6	1.5
HA Ph	2	0.4							1	0.5	7	2.1			1	0.3		
HA Sp					1	0.3					1	0.3						
LC d											1	0.3						
LC e	23	4.9	9	1.9	4	1.1	2	1.2	6	2.9	3	0.9	2	0.9	5	1.4	4	1.0
LC p	15	3.2	22	4.8	38	10.7	9	5.4	24	11.5	4	1.2	23	10.3	10	2.8	4	1.0
LC PO	40	8.6	26	5.6	21	5.9	4	2.4	16	7.7	1	0.3	11	4.9	26	7.3	16	3.9
LC v	7	1.5	5	1.1	4	1.1	1	0.6			3	0.9			2	0.6	3	0.7
LC w									1	0.5	1	0.3			4	1.1	11	2.7
P Bk p re			1	0.2											4	1.1		
P Bk p se	16	3.4	17	3.7	11	3.1	15	9.0	9	4.3	12	3.6			16	4.5	6	1.5
P Bk s re	4	0.9	4	0.9	7	2.0	7	4.2										
P Bk s se	43	9.2	89	19.5	39	11.0	58	34.7	4	1.9	18	5.4	29	13.0	21	5.9	24	5.8
P El p	40	8.6	62	13.4	25	7.0	5	3.0	10	4.8	15	4.5	35	15.7	18	5.1	24	5.8
P El s													5		1	0.3		
P El v			1	0.2														
P t p se	2	0.4	9	1.9	12	3.4	2	1.2	5	2.4	1	0.3			3	0.8	10	2.4
P t s se									3	1.4	8	2.4						
PL	110	23.6	23	5.0	59	16.6	6	3.6	8	3.8	25	7.5	25	11.2	81	22.8	196	47.6
ShC	26	5.6	26	5.6	28	7.9	13	7.8	16	7.7	4	1.2	15	6.7	38	10.7	10	2.4
ShC Bi	1	0.2	11	2.4	9	2.5	1	0.6					13	5.8	13	3.7	4	1.0
Sp e			1	0.2									7	3.1				
Sp p	4	0.9	4	0.9					2	1.0	1	0.3			1	0.3	1	0.2
Sp s	1	0.2	12	2.6	5	1.4	1	0.6	5	2.4	9	2.7	4	1.8	2	0.6	1	0.2
Sp v	1	0.2	2	0.4			2	1.2			13	3.9						
SS JS	1	0.2	1	0.2											16	4.5	26	6.3
SS LC e	1	0.2																
SS LC p	11	2.4	20	4.5	2	0.6	1	0.6	2	1.0	1	0.3	2	0.9	12	3.4		
SS LC si	1	0.2	1	0.2														
SS LC v	1	0.2													1	0.3		
SS LC w	7	1.5	3	0.6	4	1.1			2	1.0	2	0.6	6	2.7	10	2.8		
SS ni	12	2.6	2	0.4	2	0.6							5	2.2	9	2.8	5	1.2
SS Ph	3	0.6	5	1.1	1						1	0.3			4	1.1	1	0.2
SS Ph w	1	0.2	1	0.2														
SS sl			2	0.4	1	0.3									1	0.3		
SS sl & EA PR			1	0.2														
SS sl S	1	0.2																
SS Sp/E	2	0.4			2	0.6							1	0.4				
SS Sp/R	11	2.4													3	0.8	1	0.2
T	1	0.2													1	0.3		
Total	466	100	462	100	356	100	167	100	208	100	333	100	222	97	356	100	412	100
Name	RKE 6		RKE 7		RKE8		RKE11		RKE18		RK19		RKE28		RKE29		RKE30	
Variable morphology	Total	%	Total	%	Total	%	Total	%	Total	%	Total sum	%	Total	%	Total	%	Total	%
I e									8	4.1	8	1.9	4	0.3				
I p	123	14.0	219	23.4	58	12.6	47	15.7	54	28.0	23	5.6	87	5.5	102	8.1	30	7.7
I s	318	36.2	250	26.8	217	47.1	173	57.9	19	9.8	58	14.1	32	2.0	168	13.4	70	17.9
I v											135	32.8			13	1.0	6	1.5
IN	13	1.5	9	1.0	2	0.4	1	0.3					1	0.1	2	0.2	1	0.3
WM	425	48.4	456	48.8	184	39.9	78	26.1	112	58.0	188	45.6	1462	92.2	970	77.3	283	72.6
Total	879	100	934	100	461	100	299	100	193	100	412	100	1586	100	1255	100	390	100

Table 18a - Kebara cave. Phytolith morphological results from deep sounding.

KEBARA CAVE						
Name (See Table 16 for description)	*RKE38*		*RKE39*		*RKE40*	
Consistent morphology	*Sum*	*%*	*Sum*	*%*	*Sum*	*%*
C p	66	19.6	34	15.0	44	24.4
C s	37	11.0	8	3.5	6	3.3
C v	1	0.3	2	0.9		
D p	1	0.3				
E e					1	0.6
E p	2	0.6	1	0.4	3	1.7
E s	5	1.5	6	2.6	7	3.9
EA H	14	4.2	3	1.3	2	1.1
EA H foeniculum type			2	0.9	1	0.6
EA PR	12	3.6	3	1.3	2	1.1
LC e	10	3.0	18	7.9	8	4.4
LC p	35	10.4	29	12.8	33	18.3
LC PO	25	7.4	8	3.5	5	2.8
LC w	8	2.4				
P Bk p se			1	0.4	7	3.9
P Bk s se			1	0.4	9	5.0
P El p	44	13.1	27	11.9	5	2.8
P El s	3	0.9	3	1.3	2	1.1
P t p se	1	0.3	2	0.9	8	4.4
P t s se	3	0.9	1	0.4	2	1.1
PL			2	0.9	3	1.7
S	1	0.3				
ShC	25	7.4	51	22.5	15	8.3
Sp p	2	0.6	4	1.8	4	2.2
Sp s	2	0.6	1	0.4	5	2.8
SS LC p	22	6.5	6	2.6	3	1.7
SS LC w	18	5.3	13	5.7	2	1.1
SS sl			1	0.4	3	1.7
Total	**337**	**100**	**227**	**100**	**180**	**100**
	RKE38		*RKE39*		*RKE40*	
Variable morphology	*Sum*	*%*	*Sum*	*%*	*Sum*	*%*
I p	41	23.0	54	21.9	58	18.5
I s	51	28.7	56	22.7	85	27.2
IN					1	0.3
WM	86	48.3	137	55.5	169	54.0
Total	**178**	**100**	**247**	**100**	**313**	**100**

Table 18b - Kebara cave. Phytolith morphological results from West profile samples.

KEBARA CAVE				
Name (See Table 16 for description)	RKE37			RKE43
Consistent morphology	Sum	%	Sum	%
C p	1	-	7	4.8
C v	1	-	2	1.4
E p	5	-	2	1.4
E s	2	-	9	6.1
EA H			2	1.4
EA PR	8	-	4	2.7
F			2	1.4
LC e	1	-		
LC p			4	2.7
LC PO	1	-	5	3.4
LC w			1	0.7
P BK p se			1	0.7
P Bk s re			1	0.7
P Bk s se			6	4.1
P El p	3	-	3	2.0
P t p se	1	-	3	2.0
PL	2	-	68	46.3
ShC			6	4.1
Sp p			2	1.4
Sp s			2	1.4
SS JS			1	0.7
SS LC p	1	-	9	6.1
SS LC si			1	0.7
SS LC w			5	3.4
SS Sp/E			1	0.7
Total	26		147	100
Name	RKE37		RKE43	
Variable morphology	Sum	%	Sum	%
I p	16	3.3	19	1.1
I s	2	0.4	21	1.2
IN			1	0.1
WM	471	96.3	1666	97.6
Total	489	100	1707	100

Table 18c - Kebara cave. Phytolith morphological results from north-eastern sector samples.

KEBARA CAVE				
Name (See Table 16 for description)	RKE44		RKE45	
Consistent morphology	Sum	%	Sum	%
B			4	0.5
C p	15	7.4	107	14.7
C s	6	2.9		
C v	7	3.4	18	2.5
D p			1	0.1
E p			3	0.4
E s	23	11.3	21	2.9
EA H			25	3.4
EA PA			1	0.1
EA PR	6	2.9	25	3.4
LC e	1	0.5	29	4.0
LC p	7	3.4	45	6.2
LC PO	16	7.8	158	21.7
LC w	1	0.5		
P Bk p se	3	1.5	16	2.2
P Bk s re	4	2.0	9	1.3
P Bk s se	62	30.4	35	4.8
P El p	26	12.7	89	12.2
P El p ch			13	1.8
P El v			4	0.5
P t p se			6	0.8
PL	5	2.5	3	0.4
ShC	16	7.8	93	12.8
ShC Bi	2	1.0	9	1.2
Sp p	1	0.5	3	0.4
Sp s			5	0.7
Sp v	1	0.5	1	0.1
SS LC p			6	0.8
SS LC w	1	0.5		
SS sl	1	0.5		
Total	204	100	729	100
Name	RKE44		RKE45	
Variable morphology		%		%
I p	45	15.3	174	24.6
I s	171	58.0	166	23.5
IN			1	0.1
WM	79	26.8	366	51.8
Total	295	100	707	100

Table 18d - Kebara cave. Phytolith morphological results from east profile samples (Upper Paleolithic levels).

KEBARA CAVE								
Name (See Table 16 for description)	RKE1		RKE 3		RKE32		RKE34	
Consistent morphology	Sum	%	Sum	%	Sum	%	Sum	%
B	1	0.9						
C p	13	12.1	3	-	24	13.6	14	19.7
C s					20	11.3	6	8.5
C v	6	5.6			3	1.7	1	1.4
D p			1	-				
E p			1	-	3	1.7	2	2.8
E s	10	9.3	9	-	43	24.3	7	9.9
EA H	2	1.9			3	1.7		
EA PR	4	3.7	1	-	6	3.4	4	5.6
LC e	5	4.7	1	-	11	6.2	5	7.0
LC p	14	13.1	2	-	3	1.7	3	4.2
LC PO	2	1.9	1	-				
LC w	1	0.9			1	0.6		
P Bk p se					3	1.7		
P Bk s re	1	0.9	1	-				
P Bk s se	17	15.9	12	-	4	2.3	2	2.8
P El in			1	-				
P El p	1	0.9	1	-	4	2.3	11	15.5
P t p se	7	6.5	5	-	5	2.8	1	1.4
P t s se					8	4.5	1	1.4
PL	5	4.7			1	0.6		
ShBi					2	1.1	3	4.2
ShC	16	15.0	5	-	14	7.9	5	7.0
Sp e					1	0.6		
Sp p			1	-	1	0.6		
Sp s	2	1.9	2	-	17	9.6	6	8.5
SS ni			1	-				
Total	107	100	48	100	177	100	71	100
Name	RKE1		RKE 3		RKE32		RKE34	
Variable morphology	Sum	%	Sum	%	Sum	%	Sum	%
I p	8	4.7	5	8.8	41	25.9	24	25.3
I s	74	43.0	24	35.3	65	41.1	39	41.1
Iv			1	1.5				
WM	90	52.3	38	55.9	52	32.9	32	33.7
Total	172	100	68	100	158	100	95	100

Table K18e - Kebara cave. Phytolith morphological results from outside samples.

Figure 32 shows the proportions of phytoliths characteristic of grasses in the samples analyzed, as well as the average and range of grass phytolith proportions observed in the reference collection of modern bark samples. Even though the spread of values is large, we conclude that most of the grass phytoliths probably entered the cave associated with the wood burned for fuel (Albert et al., 1999b). Note that grasses produce about 20 times more phytoliths than wood per unit weight of ash AIF (Table 2 & Figure 8).

The two samples with the lowest proportions of grass phytoliths (RKE19 & RKE30) (Figure 32) are both from the brown sediments located between hearths. This low percentage is not consistent with the number observed of the grass phytolith in the bark of trees from the area. Indeed they do contain unusual consistent morphology phytoliths not found in the other hearths. This would indicate that these samples contain a relatively high proportion of phytoliths with characteristic morphologies that are not derived from wood and bark, or the grass phytoliths that are associated with wood and bark. Table 18a lists the phytolith types for these two samples.

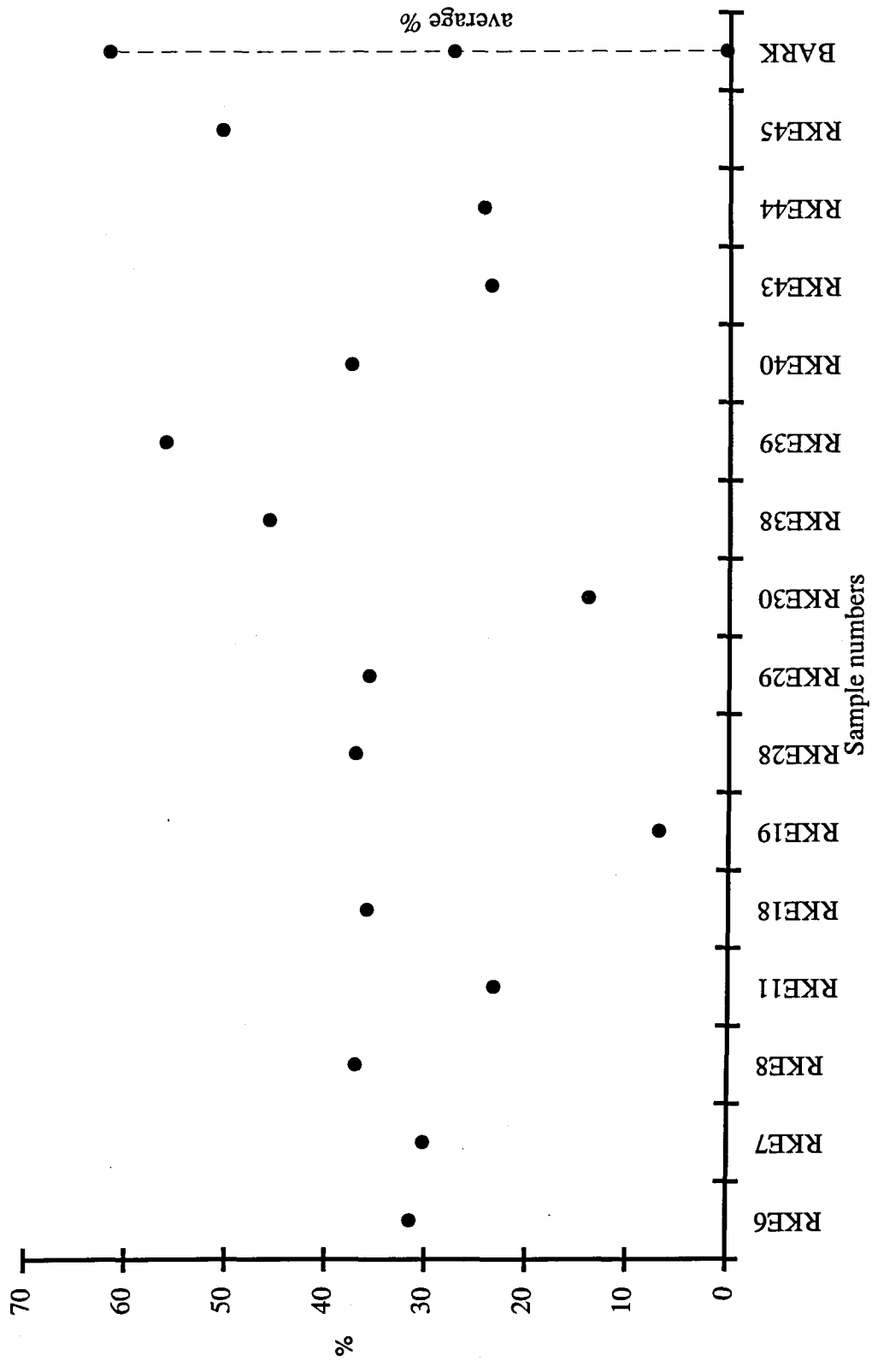

Figure 32 – Percentages of grass phytoliths in the total assemblage of consistent morphology phytoliths identified in the archaeological samples from Kebara cave. The percent range of grass phytoliths from bark identified in the reference collection of modern plant taxa from the Carmel area (Israel) is also shown. *Wood contains almost not consistent morphology phytoliths.*

In sample RKE19 the unusual phytoliths are those with verrucated surfaces (cylindroid, ellipsoid, spheroid and irregular verrucated) (Figure 33a). These are not found in the reference collection. In sample RKE30, platelets (PL) are abundant (Figure 5I showed an exemple of platelet phytolith). Platelets although generally present in the reference collection, are relatively rare. They are abundant only in the fruits of *Pinus halepensis* (54% of the consistent morphology phytoliths) (Table 5d). We therefore conclude from the analyses of these two samples that the plants containing these phytoliths were brought into the cave for purposes other than fuel for fires. For example, humans introduce plant materials for bedding as well as for food (Albert et al. 1999b).

We have noted that certain stratigraphic levels do contain phytoliths that are not found elsewhere. These are in addition to the omnipresent wood and bark derived phytoliths. For example, all 3 samples (RKE6, RKE7 & RKE8) from the lowest levels of the deep sounding have phytoliths that are characteristic of leaves. In fact, in sample RKE6 phytoliths, probably from the leaves of *Quercus calliprinos* (Kermes oak), were

identified (Figure 33b & 33c). Samples RKE29 and RKE30 also have phytoliths that are characteristic of leaves, but these are different from those at the base of the section.

They have the so-called jigsaw puzzle motif (Bozarth, 1992) (Figure 33d). Another type of hair cell derived phytolith, named the "Bozarth type", was identified in sample RKE7 (Table 18a) (Figure 33e). Bozarth identified this specific type of hair in *Cirsium ochrocentrum* (yellowspine thistle) from the Compositae family (Bozarth, 1992, p. 211). We did not observe this type of hair phytolith in the reference collection. Other unusual phytoliths present in the deep sounding, and especially in sample RKE6, but not in the reference collection, are silica skeleton spheroids with rings (Figure 33f). These phytoliths do not seem to possess the classical pattern of leaf phytoliths from woody dicotyledons or gymnosperms. They may be from other type of plants, not identified in our reference collection. It is conceivable that these plant taxa are not present in the area any longer. Dr. A. Rosen (personal communication) observed some of these forms in the Mousterian levels of Hayonim cave in the Galilee, but could also not identify the plant taxa in which these phytoliths formed. These types of phytoliths were also observed in one outside sample from Tabun cave (Figure 23c).

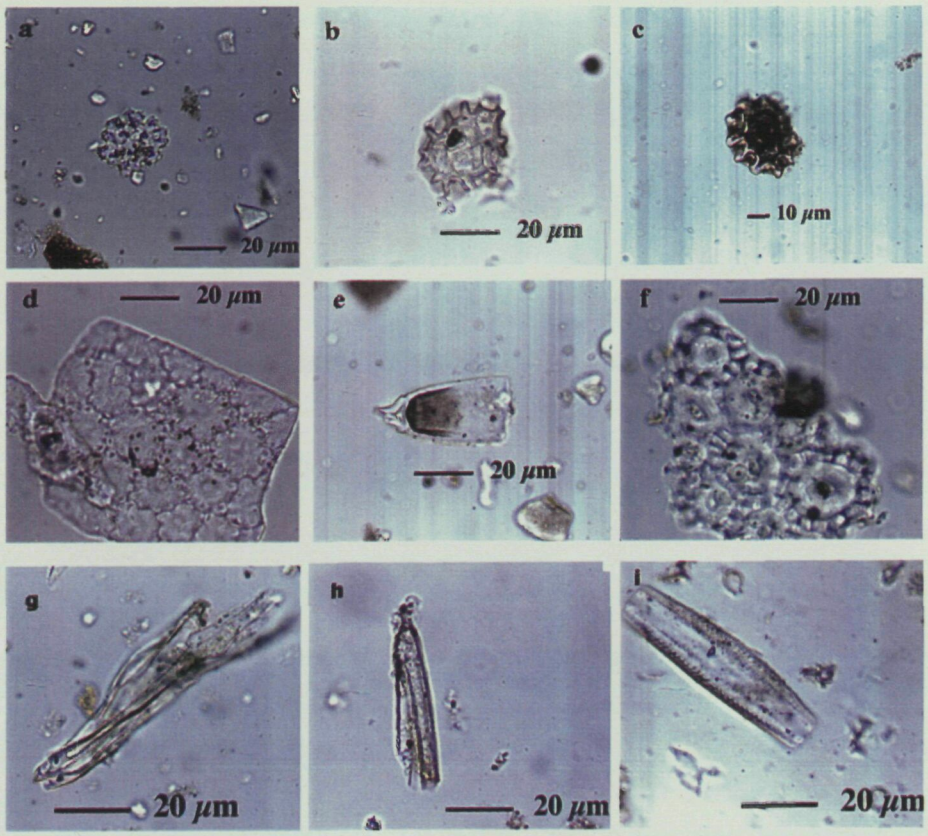

Figure 33 – Photomicrographs of phytoliths from Kebara cave and the reference collection. Pictures at taken at 400x. a) Spheroid verrucate identified in sample RKE19 (brown layer from the deep sounding). b) Silica skeleton polyhedral with wavy edges identified in the leaves of *Quercus calliprinos* (Kermes oak). c) Silica skeleton polyhedral with wavy edges identified in Kebara cave sample RKE6 at the bottom of the deep sounding. d) Silica skeleton jigsaw puzzle identified in sample RKE29 (hearth from the deep sounding). e) Hair "Bozarth type" identified in sample RKE7 from the deep sounding. f) Silica skeleton spheroid with rings identified in the sample RKE6 in the deep sounding. g) Epidermal appendage, Hair identified in *Foeniculum vulgare* (fennel) . h) Hair identified in the hearth from sample RKE39 in the west profile in Kebara cave. i) Diatom from sample RKE45 in the Upper Paleolithic level.

Samples RKE38, RKE39 and RKE40 also show some distinctive characteristics. They all belong to the same hearth complex. RKE38 and RKE39 belong to the same layer and were located a few centimeters apart. All three samples have very similar mineralogical compositions and a much lower number of phytoliths per gram of AIF compared to other samples. Samples RKE38 and RKE39 contain the highest proportion of silica skeletons from grasses and a complete absence of silica skeletons from leaves of dicotyledons (Table 18b). These samples thus have a different phytolith composition than the rest of the samples. Phytoliths with consistent morphology characteristics of wood and bark of woody dicotyledons are the most common forms identified in these samples. The exception is the presence of some epidermal appendages cells (hairs), which in samples RKE39 & RKE40 are derived from fennel (Figure 33g-h).

Sample RKE18 is most unusual. It contains mainly siliceous aggregates in the low-density fractions, which is consistent with the small number of phytoliths per gram of AIF (650,000) (Table 16). The v/c ratio of the phytoliths is relatively low (0.9) indicating that other phytoliths, in addition to those from wood/bark, are present. The micromorphological analyses carried out by P. Goldberg (personal communication)

indicated that this sample contains many seed coats, which are quite fragmentary and possibly etched. The results of our reference collection showed that, for instance, the husk of the nuts of *Quercus ithaburensis* (Tabor oak), show a low ratio between variable and consistent morphology phytoliths (0.6) and a low number of phytoliths (805,000) (Tables 2 & 3). Note that the morphologies of the phytoliths from the husk of *Quercus ithaburensis*, are the same as those present in the wood and bark, and therefore cannot be used for identifying husks in archaeological sediments.

Two brown colored samples from the Upper Paleolithic period were analyzed (RKE44 & RKE45). Although both have similar mineralogical compositions, the phytolith assemblages are quite different. Sample RKE45 contains ten times more phytoliths than RKE44 (Table 16). This sample is from the layer described by P. Goldberg (personal communication; Goldberg & Bar-Yosef, 1998) as containing fairly abundant diatoms and phytoliths, suggesting the deposition of ponded sediments. In our sample, diatoms comprised about 2% of the total number recorded (Figure 33i). The proportion of grass phytoliths in this sample is one of the highest of all the samples analyzed (Figure 32). There are many other differences in the phytolith assemblages of the two samples. These differences must reflect quite different environments of

formation. Interestingly, the presence of diatoms in RKE45 is also associated with large amounts of phytoliths with a diversity of forms, representing woody dicotyledons, grasses and non-woody dicotyledons (Albert et al. 1999b). It is difficult to determine from these observations what sort of environment must have existed at this time.

Samples from outside the cave (RKE1, RKE3, RKE32 & RKE34) are all terra rossa soils. They are all very similar, having the same major mineral components, quartz and clay, and very small amounts of phytoliths (Table 17). The phytoliths that are present are characteristic of both grasses and wood and bark. The characteristics of these samples are, in almost every respect, different from those inside the cave (Albert et al. 1999b). These samples gave similar results to those obtained from the outside samples of Tabun cave, in the number of phytoliths per 1 g of AIF, ratio v/c morphology (Table 13 & Table 16).

C) Discussion

The phytolith concentrations and assemblages in the samples from within the cave contrast markedly with those from the soils around the cave. This clearly shows

that the input into the cave of plant material, from which the phytoliths were derived, is unique to the cave environment. Furthermore, as the large majority of the cave phytoliths are derived from the wood and bark of ash that was used as fuel for fire, it can be concluded that anthropogenic activities are the major determining factor in terms of phytolith transport into the cave. Phytoliths from plant taxa not related to the use of fire were also identified, especially in those layers between hearths. The unique phytoliths are often minor components of the entire assemblage. Their presence shows that the microstratigraphy is relatively well preserved, at least in the section in the deep sounding. It also indicates that phytoliths, in this area, did not move vertically, and therefore the phytoliths remained *in situ*.

Phytolith preservation

Phytolith preservation is always a concern, particularly as silica solubility does increase as conditions become more alkaline (Iler, 1979). In this study we noted that many of the variable morphology phytoliths examined showed signs of some surface etching or partial dissolution. This implies that the variable morphology phytoliths are more soluble than the consistent morphology phytoliths. This is particularly evident in

one white ash layer (RKE28), where the dissolution seems to affect the variable morphology phytoliths and the siliceous aggregates, whereas the consistent morphology phytoliths are abundant and well preserved. We do not think that this degree of diagenesis significantly affects the distribution of phytolith types in this sample, nor in all the others with better preservation. The exceptions are the two samples that were extracted from the hearths, which today are composed mainly of calcite. These phytoliths are very poorly preserved. This is paradoxical, as these hearths in terms of mineralogy, are the best-preserved (Schiegl et al., 1996), bearing in mind that fresh wood ash is also composed mainly of calcite (Humphreys, Hunt & Buchanan, 1987). The water in chemical equilibrium with calcite has a pH of around 8.4, but under certain circumstances can be even higher (Stumm & Morgan, 1970). Thus apparently in this environment and given sufficient time, phytoliths do dissolve. Surprisingly in both these samples, the consistent morphology phytoliths seem to have preferentially dissolved as compared to the variable morphology types; something we do not understand. Thus the phytolith assemblages of these two samples are too diagenetically altered to be useful in terms of their archaeological implications.

Remains of silica, in the calcitic hearths are present in relatively large amounts per gram AIF, despite the fact that they were subjected to severe dissolution. This can be explained by postulating that the siliceous aggregates, the major component of the AIF together with quartz, also dissolved, and the silica matrix is what is left, when looking at the microscope. This is consistent with our observation that when we treated wood with oxidizing acids (the so-called "wet ashing" procedure of Piperno, 1988), what eventually remained of the mineral fraction was quartz and phytoliths. All the siliceous aggregates dissolved more rapidly than the phytoliths (unpublished observation). This suggests that at neutral to acidic pH, the phytoliths may well be the most stable biogenic components in prehistoric caves.

It should be noted that all the phytoliths in the cave must once have been located in a calcitic ash environment. Yet they did not all undergo extensive dissolution. This suggests that in most of the cave, the calcite did not survive long enough after it was formed to cause severe dissolution of the phytoliths. This is consistent with the scenario proposed by Karkanas et al. (1999) that envisages most diagenetic processes in prehistoric caves occurring rapidly either on the surface or soon after burial. They deduce from isochron data produced during thermoluminescence dating of burned flint

tools, that "rapid" is several thousand years. Apparently when calcite is preserved for more extensive periods of time under cave conditions, the phytolith assemblages are severely altered. This may have important implications for phytolith preservation in other caves, where calcite is abundantly preserved in the sediments for long periods of time.

Phytolith analyses

The detailed analyses of the deep sounding of both the phytoliths and the minerals in the sediments from above the bedrock to almost the Upper Paleolithic-Mousterian boundary show that wood ash is always the major component. Even the sediments between clearly discernible hearths are composed of ash-derived minerals. Clay is present in only minor amounts, except in areas close to the entrance. The visible hearths are not, therefore, a complete guide to the distribution of ash in the section. This confirms and amplifies previous observations by Schiegl et al. (1996).

The average proportion of grass phytoliths in all the samples is relatively low, especially when taking into account the fact that grasses produce about twenty times

more phytoliths per unit weight AIF than is present in wood and bark (Table 2 & Figure 8). Furthermore, the proportions of grass phytoliths in these samples are very similar to those obtained in modern bark. This implies that most of the grass phytoliths present in the sediment samples were probably associated with the wood and bark fuel burned in the fires, and do not imply that grass was a major fuel component of these fires. It is interesting to note that in Tabun cave level B, what is roughly the same age as the Kebaran Mousterian sediments, only wood/bark phytoliths were observed and no grass (Table 14a). It has been suggested that the immediate area above Tabun cave was heavily wooded. However it has to be taken into account the low amount of phytoliths with consistent morphology recovered from this level.

We noted that the two samples of sediments between hearths, both contained the lowest proportions of phytoliths characteristics of grasses (Figure 32). Each of the samples also contained phytoliths from plants whose identities remain unknown. These apparently "diluted" the ash derived phytolith components. Although two samples are clearly insufficient to draw definitive conclusions, this observation does suggest that other plants were brought into the caves in relatively large amounts (or in small amounts, but they happened to have high concentrations of phytoliths), for purposes unrelated to

providing fuels for fire. This is especially true for sample RKE19 where the phytolith composition is completely different from the rest of the samples. The presence of plant remains associated with food was previously observed by Lev & Kislev, (1993). They found most of the edible remains near the hearths. Other possible purpose for the introduction of plant remains in the cave could be for bedding. These remains should also be found near the hearths.

One unexpected observation is that the two samples from the oldest sediments of the deep sounding (RKE6 & RKE7) contain, for the most part, phytoliths derived from wood and bark, as well as other phytolith types not from wood and bark. They also contain siliceous aggregates and the two phosphate minerals, leucophosphite and montgomeryte, which are thought to be derived from the original ash calcite. Thus from the phytolith and mineralogical analyses we conclude that fires were made in the cave at this time, although other plant remains, maybe not related with fire were also present. These layers, however, did not produce any stone artifacts, and were therefore described as "sterile" (Bar-Yosef et al., 1992). The paradox may be more apparent than real, due to the fact that these basal layers were only exposed over a very small area at the bottom of the deep sounding and this area happened not to yield stone artifacts.

The hearths in Kebara cave when viewed in section often comprise a white or yellow colored upper layer, and a black or dark brown lower layer, with the latter clearly having more organic material. It therefore seems that this is the product of fires made in the same place. We analyzed the white and black layers of one hearth separately (samples RKE28 & RKE29) and found significant differences in mineralogy, v/c ratios and phytolith assemblages. Part of the difference between the black and white layers of the same hearth are due to preservation. The white layer being more poorly preserved than the black (almost no phosphate minerals, fewer siliceous aggregates, and more phytoliths showing signs of weathering). Despite this, there are significant differences in consistent morphology phytolith assemblages between the two. Phytoliths characteristic of leaves and non-woody dicotyledons are more abundant in the black layer (almost 12%) than in the white layer (less than 4%) (Figure 34). The black layer contains several types of silica skeletons that are almost absent in the white layer. These silica skeletons indicate the presence of grasses (SS LC), leaves of woody dicotyledons (SS Ph & SS Sp) and the presence of other non-woody dicotyledons plant taxa (SS SP/R) (Table 18a). Clearly the black layer is not simply the charcoal-rich portion of the ash produced in these fires. These differences may reflect a time sequence of ash accumulation. More detailed studies of this type are necessary.

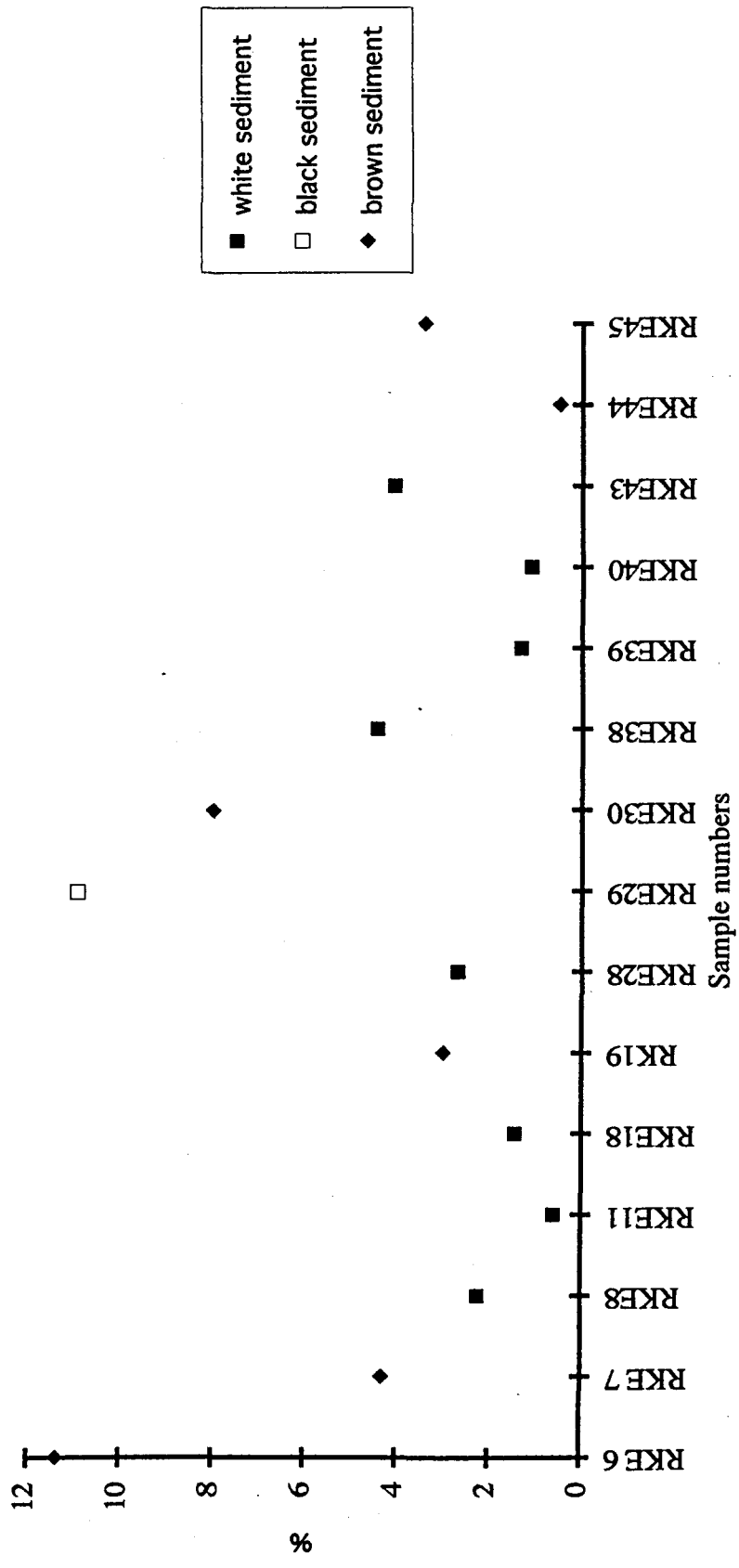

Figure 34 – Percentages of phytoliths from leaves of woody and non-woody dicotyledons identified in the archaeological samples from Kebara cave.